THE AMERICAN MINERALOGIST
JOURNAL OF THE MINERALOGICAL SOCIETY OF AMERICA

Vol. 20 JULY, 1935 No. 7

THE STRUCTURAL RELATIONSHIP OF NONTRONITES AND MONTMORILLONITE

JOHN W. GRUNER, *University of Minnesota, Minneapolis, Minn.*

INTRODUCTION

Nontronites have been regarded quite often as iron kaolinites, though some investigators (1) are inclined to group them among the zeolites. On account of the extremely fine-grained nature of all the nontronites the only hope for the solution of this problem lies in the investigation by means of *x*-rays. By the use of the powder method the writer will show that nontronites including morencite, pinguite, faratsihite, stilpnochloran and chloropal are like montmorillonite in structure. They are, therefore, layer structures, very similar to vermiculites but unlike kaolinite. They have no resemblance to the structures of zeolites.

The writer wishes to express his thanks to Mr. Russell Wayland for his assistance in measuring and calculating over forty films, and to the Graduate School of the University of Minnesota whose grants made this study possible. He is also indebted to Dr. W. F. Foshag and Dr. E. P. Henderson of the United States National Museum for most of the specimens investigated.

MINERALS USED

1. Nontronite, Peta Luma, California. United States National Museum specimen. Greenish lemon yellow veinlets in a reddish brown decomposed brecciated rock. Contains considerable amounts of calcite.
2. "Morencite," Arizona Central Mine, Morenci, Arizona. United States National Museum specimen No. 86033. Described by W. Lindgren and W. F. Hillebrand, *Am. Jour. Sci.*, vol. **18,** p. 455, 1904. Sample used contains a little quartz and some unidentified impurities.
3. "Faratsihite," Faratsiho, Madagascar. United States National Museum No. 95754. Described by M. A. Lacroix, *Bull. Soc. Mineral.*, vol. **37,** p. 231, 1914.
4. Nontronite, White Oak Creek about three miles east of Bakersville, North Carolina. Received from E. P. Henderson, United States National Museum. Contains some brownish stains.
5. "Pinguite," Geilsdorf, Saxony. United States National Museum No. R4881. Greenish lemon yellow, compact.
6. "Stilpnochloran," Gobitschau, Moravia. Light brown fibrous-looking material.

This specimen was obtained through the kindness of Dr. Julius Holzner who described it in two papers (see references).

7. Nontronite, Mt. Magnitnaya, Ural Mountains. Mixed with other silicates. Greenish yellow, fibrous looking. The powder photograph of this nontronite is not included in table 1 on account of a number of lines belonging to impurities.
8. Montmorillonite ("bentonite"), unknown locality. Dense pinkish white specimens.

X-RAY DATA

Of all the layer structures investigated by the writer nontronites and montmorillonite yield the poorest powder spectrum photographs. This is undoubtedly due chiefly to the extremely small size of the individual particles. It may also be caused by a certain lack of parallelism of layers in individual "books." This absence of parallelism would exist in addition to common block structure phenomena and could be due to distortion in the layers themselves or unequal distribution of H_2O content between them.

Though the lines are broad and diffused they are good enough to give the interplanar distances (d) and intensities (I) recorded in table 1. Fe radiation from a modified Ksanda ion tube was used. Exposures were twenty-four hours at 10 MA and 30 KV. The radii of the cameras were 57.3 mm. The powders mounted on silk threads with collodion were not over 0.8 mm. in diameter. Montmorillonite was x-rayed in the same manner and its lines (given in table 1) agree with the powder spectrum photograms of other investigators of montmorillonite (5, 9, 10). Certain changes in the lines of nontronites occurred when the minerals were partially dehydrated over periods of thirty hours at 300°C. The essential changes are recorded in table 1. The distances for which no changes are indicated remained practically unaltered in the dehydrated material. The same statement applies to specimens almost completely dehydrated at 575°C. (twenty hours heating in air).

Three samples were x-rayed after their powders had been placed in water for four days. An attempt was made to keep the powders moist by means of a wick in contact with the mounting threads during the exposure.* That the attempt was successful is shown in table 1 by the increases of the distances for lines No. 1. It was not possible, however, to ascertain the amount of H_2O in the powders actually x-rayed.

---

* Glass tubes could not be used for containers of these moist powders because Fe radiation is largely absorbed by the glass.

INTERPRETATION OF DATA

The agreements between the lines of the nontronites and montmorillonite are obvious in table 1, that is if one makes allowance for the difference in the sizes of the Al and Fe'' ions. The agreement is even more striking in a comparison of the films themselves which, however, do not lend themselves well to photographic reproduction.

Hofmann, Endell and Wilm (5) have given us an interpretation of the montmorillonite structure with which the writer agrees except for some of the indices they assigned to their reflections. According to them montmorillonite is built up of layers as pyrophyllite and talc (6) with this difference, however, that H_2O is present between the layers. The distance between centers of layers is determined by the amount of H_2O available. Under water, for example, it is as high as 19.6 Å. The spacing, therefore, is entirely dependent on the percentage of H_2O in the specimen. The writer has shown a similar structure for vermiculite (this journal, vol. **19**, p. 571, figs. 1 and 2) with this difference, however: The spacing appears to be constant (14.2 Å) over a wide range of H_2O content. It decreases to that of talc (9.2 Å) at some relatively high temperature. It has not been possible so far to fix this temperature definitely.

Since the basal pinacoid reflections seem to be the only ones which alter their positions with changing H_2O in montmorillonite, Hofmann, Endell and Wilm assume that the unit cell is orthorhombic and assign (hk0) indices to the stationary reflections. It is doubtful whether they are correct in their assumption, for montmorillonite lines are too diffuse to measure them very accurately. If the cell is monoclinic as found for all similar structures, the reflections might still appear unchanged after contraction of the lattice. Table 1 illustrates this point for nontronites. Leaving basal reflections out of consideration only a few essential changes occur. The other reflections also seem to show shifts but of insignificant magnitude when considering such poorly crystallized material.

The dimensions of the unit cell of nontronite, averaging the first six specimens of table 1, would be, on the basis of hexagonal SiO_4 layers, $a_0 = 5.23$ Å and $b_0 = 9.06$ Å. The values for montmorillonite are correspondingly smaller. The distance $d_{(002)}$ for laboratory-dry material varies between 12.4 and 14.7 Å, depending on the amount of H_2O. Since the angle β is unknown, c_0 cannot be evaluated. It is probable that the unit cell is two layers high as it is in most of

TABLE 1
POWDER DIAGRAMS OF NONTRONITES, FE RADIATION

No.	1		2		3		4		5		6		Paulusbrunn*		Montmorillonite		Indices
	d	*I*	*d*	*I*	*d*	*I*	*d*	*I*	*d*	*I*	*d*	*I*	*d*	*I*	*d*	*I*	
1	14.7	7–8	12.4	3	13.9	4	13.9	6	14.1	8–10	13.4	5–8	Obscured by arrangement of camera		15.0	8	200
2			7	*ind*	7.1	1 *ind*	7	*ind*									
3	4.93	1*β*	4.95	0.5*β*	4.87	0.5*β*	4.97	1*β*	5.02	1*β*	4.99	0.5*β*			4.92	1*β*	
4	4.48	3	4.48	2–3	4.44	3	4.50	4	4.55	3–4	4.51	3	4.56	*st*	4.45	3	
5	4.26	0.5 *ind*	4.14	1	3.94	0.5 *ind β*					4.18	1	4.12	*ss*			
6			3.55	1	3.54	2	3.42	1–2					3.52	*ss*			
7													3.13	*s*			
8			2.84	0.5	2.79	0.5	2.80	0.5	2.80	0.5–1	2.82	0.5	2.82	*s*	2.81	*ind*	
9	2.72	0.5	2.68	1							2.68	0.5					
10	2.571	1–2	2.573	1–2	2.588	1–2			2.584	2	2.577	2	2.562	*mst*	2.535	2	
11	2.476	1–2	2.501	1–2	2.507	1 *ind*	2.521	2 *vb*									
12			2.437	1–2							2.436	2	2.436	*ss*	2.43	*ind*	
13	2.267	0.5	2.259	0.5–1	2.272	0.5 *vb*	2.2	*ind*	2.28	*ind*			2.242	*ss*	2.228	0.5	
14			2.180	0.5–1							2.180	0.5–1 *vb*					
15			2.071	0.5									2.115	*ss*			
16	2.046	0.5	1.995	0.5–1													
17	1.859	1	1.884	0.5					1.862	0.5	1.888	0.5–1	1.884	*ss*	1.851	0.5	
18	1.795	0.5											1.808	*ss*			
19			1.712	1–2	1.720	0.5–1	1.716	0.5–1	1.718	1			1.739	*s*			
20	1.701	0.5									1.708	1–2	1.690	*s*	1.688	1	
21	1.657	0.5	1.659	1	1.678	1	1.670	1	1.670	1	1.665	1–2			1.643	1	
22	1.618	0.5			1.632	0.5–1	1.629	0.5									
23			1.560	0.5							1.556	0.5	1.583	*ss*			
24	1.500	2*b*	1.506	2–3	1.519	2	1.517	3	1.517	3–4	1.505	4	1.528	*st*	1.494	3	060
25					1.481	2	1.478	1									
26	1.462	0.5	1.449	0.5	1.451	0.5					1.444	0.5	1.450	*ss*	1.415	0.5	
27	1.409	0.5	1.391	0.5					1.390	0.5			1.401	*ss*			
28	1.345	0.5											1.363	*ss*			
29					1.307	0.5	1.305	1 *b*	1.304	0.5–1	1.299	0.5	1.314	*s*	1.285	1	
30	1.284	0.5–1 *b*			1.281	0.5	1.282	0.5	1.280	0.5							
31			1.253	0.5–1	1.263	0.5–1	1.260	1	1.263	1	1.254	0.5	1.268	*s*	1.241	0.5	
32	1.236	0.5			1.231	0.5–1											

TABLE 1 (*Continued*)

Essential Changes After Heating at 300°C.

No.	1		2		3		4		5		6		Paulusbrunn*		Montmoril-lonite		Indices
	d	*I*	*d*	*I*	*d*	*I*	*d*	*I*	*d*	*I*	*d*	*I*	*d*	*I*	*d*	*I*	
1	14.0	2	disappeared		disappeared		disappeared		13.8	4–5	disappeared						002
1*a*	none		9.87	2–3					9.90	1	9.56	2–3			9.8#		002
7*a*	none		3.169	2 *b*	3.085	*ind*	none		3.118	1	3.123	3					
11*a*	*ind*		2.514	2–3	2.498	2 *b*	2.472	1 *vb*	2.476	1 *vb*	2.496	2					

Essential Changes After Dehydration at 575°C.

No.	1		2		3		4		5		6		Paulusbrunn*		Montmoril-lonite		Indices
1*a*	9.72	2	9.56	4	9.61	2	9.17	2	9.37	3	9.37	3			9.6#		002
7*a*	3.160	2	3.169	3	3.126	2	3.107	2	3.134	3	3.126	3					
11*a*	2.466	1 *vb*	2.517	2–3	2.462	1 *vb*	2.447	1 *vb*	2.475	1 *vb*	2.47	*ind*					
			2.452	1 *vb*													

Essential Changes When X-rayed While Moist

No.	1		2		3		4		5		6		Paulusbrunn*		Montmoril-lonite		Indices
1	15.8	6			15.8		14.9										002

β = line definitely caused by K_β radiation.
b = outer edge of broad line.
vb = outer edge of very broad line.
ind = indistinct edge of line.
* Diagram by Noll (1). *st* = strong, *s* = weak, *ss* = very weak, *m* = medium.
# After Hofmann, Endell and Wilm (5).

the other layer-structures. The density determinations of nontronites are unreliable on account of the fluctuations of the distances between layers. They should, however, be greater than 2.2 for laboratory-dry material.

CHEMICAL CONSIDERATIONS

One finds little encouragement in the perusal of the chemical mineralogy of nontronites. The analyses vary between very wide limits, and different mineral names apply to the same species. It is certain now that nontronite, morencite, pinguite, chloropal (1), faratsihite, and stilpnochloran are structurally identical and should be called nontronite though faratsihite might just as well be classed as beidellite according to its analysis in table 2. Four analyses are given in this table. While specimens Nos. 2 and 3 come from the type localities, it is probable that the samples *x*-rayed would not be exactly like the analyzed material of table 2. Stilpnochloran No. 6 is exactly like the *x*-rayed material according to Dr. J. Holzner who had suspected* that it is nontronite. The water content might be different, however, due to a change in climatic conditions. In connection with this material the findings of Holzner (3 and 4) that it absorbs large amounts of thallium are very interesting. Thallium replaces calcium and water according to Holzner.

The unit cell of the proposed structure of nontronite (for illustration see this journal, vol. **19**, p. 571, fig. 2) contains 16 Si positions of which four or even more could be occupied by Al, as in the micas. It also has 8 to 12 (Al, Fe‴, Fe″, Mg) positions between the Si_4O_{10} layers. The total number of occupied cation positions then is somewhere between 24 and 28. If *for the present discussion we consider the small amounts of Fe″ and Mg trivalent* the number will be close to 24. If just 12 positions of the 16 possible ones were occupied by Si, table 2 shows how many positions would be occupied by available (Fe‴, Al Fe″ Mg) ions. There is evidently a deficiency of such ions unless Si occupies from 12.5 to 14 positions.† If we make the further assumption—which is reasonable—that the number of O and OH ions is fairly constant in the structure, we arrive at the following structural formula:

$$OH_8(Fe''', Al)_{8+n/3}(Si_{16-n}(Al, Fe''')_n)O_{40}\cdot mH_2O.$$

---

* Written communication.

† Note the similarity to glauconite in this respect (8).

TABLE 2

ANALYSES AND ATOMIC DISTRIBUTION

					No. of Ions in Unit Cell			
	2	3	6	Paulus-brunn*	2	3	6	Paulus-brunn*
SiO_2	45.74	41.60	36.45	40.02	12.0	12.0	12.0	12.0
TiO_2	trace	.13	0.02	—	(14.1)	(12.8)	(12.8)	(13.5)
Al_2O_3	1.98	22.68	6.03	10.55				
Fe_2O_3	29.68	15.22	34.24	26.16	8.7	11.4	11.2	10.0
FeO	0.83	0.54	none	1.37	(10.5)	(12.2)	(12.0)	(11.3)
MgO	3.99	0.11	0.97	—				
CaO	1.61	0.60	1.91	—				
MnO	trace	—	0.04	—				
K_2O	0.20	0.22	0.35	—				
Na_2O	0.10	0.16	none	—				
H_2O-	8.84	5.71	11.01	13.25	12.2	18.0	22.2	21.8
H_2O+	5.08	13.02	9.20	8.58	(14.3)	(19.2)	(23.7)	(24.5)
FeS_2	0.66	—	—	—				
P_2O_5	0.18	0.21	0.31	—				
Total	98.89	100.20	100.53	99.93				
Sp. Gr.	—	2.523	—	—	n=1.9	n=3.2	n=3.2	n=2.5

2. Lindgren and Hillebrand, analysts.
3. M. A. Lacroix, analyst.
6. J. Holzner, analyst.
* W. Noll, analyst.

Based on this formula the calculated numbers of ions in a unit cell for the analyzed samples are recorded as numbers in parentheses in table 2; n values are also given. In general, then, the value of n lies between 1 and 4 and that of m between 8 and 22 for air-dried nontronite. The same formula may be used for the isomorphous montmorillonite in which case n approaches zero. Beidellite which according to Larsen and Steiger (2, p. 18) is very similar to nontronite would have a value of n between 1 and 3. As a matter of fact the analysis No. 3 of faratsihite approaches beidellite more closely (2, p. 15) than nontronite. No other beidellite was available to the writer.

It appears from all the available information that the capacity for giving off and reabsorbing water between the layers is greatest in montmorillonite in which $n=0$ or close to 0. It might be thought then that the occupation of 16 Si positions by Si is the deciding factor. On the other hand, the Al: Fe''' ratio may control the absorption process—that is, the more Al present the greater the capacity for H_2O when the mineral is kept moist. It is hoped to continue this phase of the study when more analyzed material is available.

On account of its similar formula hisingerite from several localities was *x*-rayed. It gives about five broad, indistinct bands which agree with the most intense lines of nontronite except for line No. 1 which could not be identified in hisingerite. The amorphous character of the mineral, therefore, seems to be established.

CONCLUSIONS

An *x*-ray investigation of nontronite, morencite, pinguite, faratsihite, chloropal, and stilpnochloran shows that these so-called species are structurally identical. It is highly probable that beidellite, hoeferite, müllerite and graminite according to Larsen and Steiger also have the same structure.

The structure is practically identical with that of montmorillonite (bentonite). Therefore, montmorillonite, beidellite, and nontronite form an isomorphous completely miscible series. As in montmorillonite the H_2O content of nontronites may fluctuate. Since they are layer structures the H_2O content controls the distances between layers. These distances vary between 9.2 Å at 575°C. and 15.8 Å if the sample is kept moist during *x*-ray exposure. The dimensions for a_0 and b_0 average 5.23 Å and 9.06 Å, respectively. When dehydrated at 575°C. nontronite is very similar to pyrophyllite in structure. The structural formula of this series is probably best expressed as follows:

$$OH_8(Al,\ Fe''')_{8+n/3}(Si_{16-n}(Al,\ Fe''')_n)O_{40}\cdot mH_2O.$$

This is based on the assumption that O and OH are constant and the small amounts of Mg, Fe'' are counted in as trivalent. The value of n will be between 0 and 4. Since the composition of these isomorphous mixtures depends largely on their environment during formation, n for nontronites probably is rarely much below 2, and may be as high as 4. For montmorillonite on the other hand n will usually be smaller than 1. The value of m lies between 8 and 22 for air-dried material.

Hisingerite appears to be amorphous. The four or five indistinct bands visible in the films agree, however, with the intense lines of nontronite.

REFERENCES

1. Noll, W., *Chemie der Erde*, vol. **5,** pp. 373–384.
2. Larsen, E. S., and Steiger, G., *Am. Jour. Sci.*, vol. **15,** p. 1, 1928.
3. Holzner Julius, *Centralblatt f. Min.*, pp. 250–56, **1934.**
4. Holzner, Julius, *Centralblatt f. Min.*, pp. 299–305, **1934.**
5. Hofmann, K., Endell, K., and Wilm, D., *Zeit. f. Kryst.*, vol. **86,** pp. 340–348, 1933.
6. Gruner, J. W., *Zeit. f. Kryst.*, vol. **88,** pp. 412–419, 1934.
7. Gruner, J. W., *Am. Mineral.*, vol. **19**, pp. 557–575, 1934.
8. Gruner, J. W., *Am. Mineral.*, vol. **20,** in press.
9. Hendricks, S. B., and Fry, W. H., *Soil Science*, vol. **29,** p. 467, 1930.
10. Kerr, P. F., *Am. Mineral.*, vol. **17,** p. 192, 1932.
11. Doelter, *Handbuch der Mineralchemie*, vol **11**, Part 2, p. 149.

LINDGRENITE, A NEW MINERAL

Charles Palache, *Harvard University, Cambridge, Mass.*

Summary

Lindgrenite is monoclinic, holohedral. $a:b:c = 0.5941:1:0.5124$; $\beta = 92°12'$. The crystals are green and transparent, tabular parallel to (010), which is a perfect cleavage. Unit cell: $a_0 = 8.45$, $b_0 = 14.03$, $c_0 = 7.04$; $\beta = 92\frac{1}{2}°$; containing Cu_{12} (MoO_4) H_8O_8. $H = 4\frac{1}{2}$. $G = 4.26$. Biaxial negative; $z = b$; $X:c = 7°$ in the acute angle β. $\alpha = 1.930$, $\beta = 2.002$, $\gamma = 2.020$; $2V = 71°$; $r > v$. Analysis: CuO 40.62, MoO_3 50.97, H_2O 3.30, Fe_2O_3 1.43, Insol. 3.34; Sum 99.66; giving $2CuMoO_4 \cdot Cu(OH)_2$. Soluble in HCl and in HNO_3. Occurs in veinlets in limonitic quartz from Chuquicamata, Chile. Named in honor of Professor Waldemar Lindgren.

The mineral described in this paper was found in a collection of ore specimens made from the oxidized zone of the great copper deposit of Chuquicamata, Chile, by Mr. M. C. Bandy, who brought them to the Harvard Mineralogical Laboratory for study. There are two specimens only in the collection: one, massive platy material interspersed in a mass of hematite; the other, a vein in limonitic quartz with many crystal-lined cavities. The crystals are in the

Table 1

Lindgrenite. Two-Circle Measurements

Forms	Crystals	Faces	Mean		Range		Quality
			ϕ	ρ	ϕ	ρ	
c 001	8	8	90°00′	2°15′	—	2°09′– 2°18′	Fair
b 010	14	28	0 00	90 00	—	—	Good
a 100	14	28	90 00	90 00	—	—	Excellent
k 120	1	1	40 32	90 00	—	—	Poor
m 110	3	4	59 18	90 00	58°41′–60°19′	—	Fair
n 210	3	4	73 07	90 00	72 39 –73 39	—	Fair
h 012	3	5	8 24	14 39	7 56 – 9 31	14°20′–14°49′	Poor
e $\bar{1}01$	1	2	−90 28	39 31	90 00 –90 28	39 30 –39 31	Poor
p 111	1	2	60 03	46 14	59 57 –60 09	—	Very poor
q $\bar{1}13$	3	5	−56 05	16 57	−55 32 –56 37	16 45 –17 15	Poor
o $\bar{1}11$	4	6	−58 09	44 11	57 58 –58 18	44 04 –44 14	Fair
r 121	12	22	41 18	53 47½	41 08 –41 28	53 31 –53 58	Excellent
s $\bar{1}21$	1	2	−38 42	52 51	38 37 –38 46	52 48 –52 54	Poor
t $\bar{1}31$	9	15	−28 13½	60 10	28 07 –28 23	59 58 –60 21	Excellent

TABLE 2
LINDGRENITE. ANGLE-TABLE

Monoclinic, holohedral.

$a:b:c=0.5941:1:0.5124; \beta=92°12'$
$p_0:q_0:r_0=0.8625:0.5120:1; \mu=87°48'$
$r_2:p_2:q_2=1.9531:1.6846:1$
$p_0'=0.8631, q_0'=0.5124, x_0'=0.0384$

Forms		ϕ	ρ	ϕ_2	$\rho_2=B$	C	A
c	001	90°00′	2°12′	87°48′	90°00′	0°00′	87°48′
b	010	0 00	90 00	90 00	0 00	90 00	90 00
a	100	90 00	90 00	0 00	90 00	87 48	0 00
k	120	40 06½	90 00	0 00	40 06½	88 35	49 53½
m	110	59 18	90 00	0 00	59 18	88 06½	30 42
n	210	73 28	90 00	0 00	73 28	87 53½	16 32
h	012	8 31½	14 31½	87 48	75 38½	14 21½	87 52
e	$\bar{1}01$	−90 00	39 31	−50 29	90 00	41 43	129 31
p	111	60 23	46 02½	47 58	69 10	44 08	51 35½
q	$\bar{1}13$	−55 35	16 49	−76 00	80 35½	18 40	103 48½
o	$\bar{1}11$	−58 09	44 09½	−50 29	68 26	46 02	126 16½
r	121	41 20½	53 46½	47 58	52 43½	52 20	57 48½
s	$\bar{1}21$	−38 49½	52 45½	−50 29	51 40	54 09½	119 56½
t	$\bar{1}31$	−28 13	60 10½	−50 29	40 08½	61 14	114 13

main thin plates, with brilliant facets on their edges. The plates reach a maximum diameter of about 4 mm.; many are much smaller and they are all very thin. They are perfectly transparent and of a green color, deep green in the thicker tablets, yellow-green in the thinner ones.

The monoclinic character is not at first apparent, since most of the crystals show under the lens a pseudo-orthorhombic symmetry, illustrated in figure 1. Measurement of the crystals, however, reveals a distribution of forms which, as exhibited in the stereographic projection, figure 6, establishes their monoclinic symmetry. Fourteen crystals were measured with the results shown in table 1. The choice of the vertical zone was determined by the invariable presence of a pair of faces of perfect quality at right angles to the dominant pinacoid (010). This was selected as the orthopinacoid (100). A face, generally small but of good average quality, was found to lie in the orthodome zone at an angle of 87°45′ to the orthopinacoid and, when this was taken as the basal pinacoid, the other forms present gave a symmetrical distribution about the vertical axis. Besides these pinacoidal forms only two others are prominently developed. These are pyramids giving excellent measurements which lead to the symbols (121) and ($\bar{1}$31). The elements were calculated from these five forms, and from these elements were derived the angles in table 2.

As shown in table 3, the agreement of the calculated and measured position angles for the principal forms is highly satisfactory.

Table 3

Lindgrenite. Calculated and Measured Angles

Forms		Calculated		Measured		Faces	Crystals
		ϕ	ρ	ϕ	ρ		
c	001	90°00′	2°12′	90°00′	2°15′	8	8
b	010	0 00	90 00	0 00	90 00	28	14
a	100	90 00	90 00	90 00	90 00	28	14
r	121	41 20	53 46½	41 18	53 47½	22	12
t	$\bar{1}$21	−28 13	60 10½	−28 13½	60 10	15	9

For the other forms, most of which were developed either as very narrow line faces or as minute dots, the measurements were less satisfactory; in general, however, they are in good agreement with the calculated angles. The variation from the mean of all measured angles for each form is shown in table 1.

The range of habit is shown in the figures. A tabular habit parallel to (010) is predominant, and generally there is an elongation more or less pronounced in the direction of the vertical axis. Doubly terminated crystals, as shown in figures 2 and 3, are rare; for the most part the crystals are attached to the cavity walls by a surface normal to the vertical axis. The very smallest crystals are slender needles of square cross section, and these often show a pronounced monoclinic termination as illustrated in figure 4. Another feature revealing monoclinic symmetry is a striation, generally visible on the clinopinacoid, which is parallel to the edge of the negative pyramid. This striation sometimes merges into a gentle curved surface inclined to the pinacoid but a few degrees

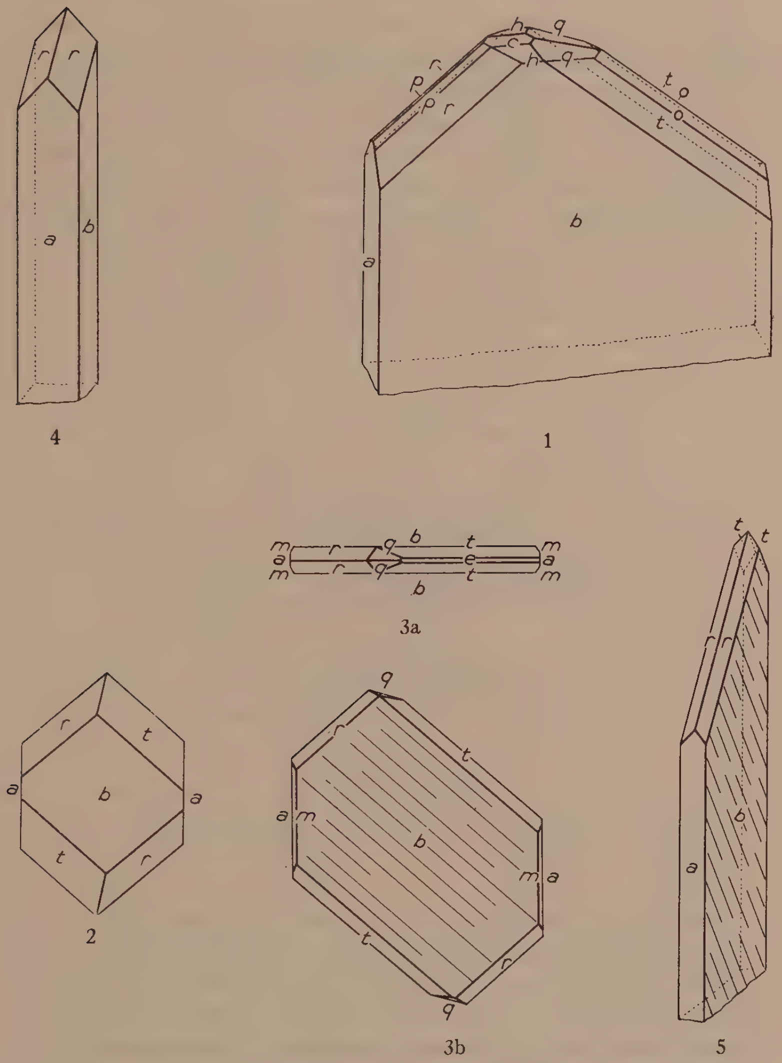

4 1

3a

2 3b 5

FIGS. 1–5. Crystals of lindgrenite.

and regarded as a vicinal development of that form. One measurement yielded the symbol ($\bar{1}$.21.1).

	φ	ρ
($\bar{1}$.21.1) measured	—4°22′	84°41′
calculated	—4 23	84 42

The prism zone, except for the two pinacoids *b* and *a*, is very weakly developed. The three prism forms listed were observed on but few crystals and always as line faces.

The clinodome *h*(012) generally accompanies the base *c*, but on one or two crystals replaces that form and on others is lacking.

The orthodome *e*($\bar{1}$01) and the pyramids *o*($\bar{1}$11) and *s*($\bar{1}$21) form a zone of line faces between the two faces of the dominant negative pyramid *t*($\bar{1}$31). None of them is prominent on the crystals.

Similarly the positive pyramid *p*(111) is a weak line form beveling the edge between two faces of the strong form *r*(121).

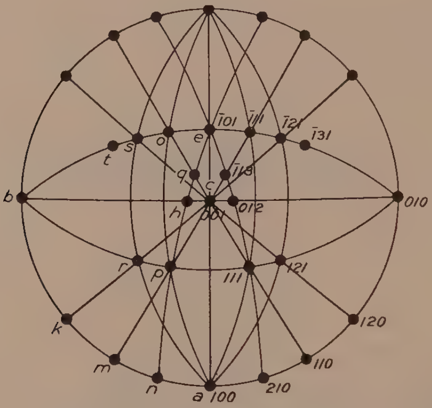

FIG. 6. Stereographic projection of the forms of lindgrenite.

The negative pyramid *q*($\bar{1}$13) was found on several crystals with distinct faces but so minute as to give poor measurements.

It was found that either *r*(121) or *t*($\bar{1}$31) may be present without the other and, unless the striation above mentioned parallel to the edge of *t* was visible, it is impossible without measurement to distinguish them. Either one gives rise occasionally to a pronounced monoclinic development of the plates as shown in figures 3 and 5. The crystal drawings are the work of Dr. M. A. Peacock.

Table 4 gives the combinations seen on the measured crystals. Twinning was not observed.

X-RAY MEASUREMENTS:—The dimensions of the structure cell were determined by Mr. Berman. Weissenberg photographs of the

TABLE 4

LINDGRENITE. COMBINATIONS OF FORMS

	c	*b*	*a*	*k*	*m*	*n*	*h*	*e*	*p*	*q*	*o*	*r*	*s*	*t*	
1	x	x	x	—	—	—	—	—	—	—	x	x	—	x	
2	x	x	x	—	—	—	—	—	x	—	x	x	—	x	
3	x	x	x	—	—	—	x	—	x	x	x	x	—	x	fig. 1
4	x	x	x	—	—	x	—	—	—	—	—	x	—	—	
5	—	x	x	—	—	—	—	—	—	—	—	x	—	x	fig. 2
6	x	x	x	x	—	x	—	—	—	x	—	x	—	x	
7	x	x	x	—	—	—	x	—	—	x	x	x	—	x	
8	—	x	x	—	x	—	—	x	—	x	—	x	—	x	fig. 3
9	—	x	x	—	x	—	x	—	—	x	x	x	—	x	
10	x	x	x	—	—	—	x	x	x	x	—	x	—	x	
11	—	x	x	—	—	—	—	—	—	—	—	x	—	—	fig. 4
12	—	x	x	—	—	—	x	—	—	x	x	x	—	x	
13	x	x	x	—	—	—	—	—	x	—	x	x	x	x	
14	—	x	x	—	—	—	—	—	—	—	—	x	—	x	fig. 5

zero layer line, with the *b*- and *c*-axes as rotation axes, checked by three rotation photographs, gave the values:

$$a_0 = 8.45\ \text{Å},\ b_0 = 14.03\ \text{Å},\ c_0 = 7.04\ \text{Å};\ \beta = 92\tfrac{1}{2}°.$$

The ratio of the cell sides:

$$a_0 : b_0 : c_0 = 0.602 : 1 : 0.502;\ \beta = 92\tfrac{1}{2}°.$$

is in fair agreement with the more accurate, previously determined morphological axial ratio:

$$a : b : c = 0.5941 : 1 : 0.5124;\ \beta = 92°12'$$

The *b*-axis zero layer line photograph shows conclusively that the morphological axial directions are also the most suitable for the structure lattice.

PHYSICAL AND OPTICAL PROPERTIES:—The cleavage of lindgrenite is perfect parallel to (010); very imperfect cleavages were observed parallel to (001) and ($\bar{1}01$). The hardness is $4\frac{1}{2}$. The specific gravity is 4.26, determined by the pycnometer (Gonyer) and by suspension in Clerici solution (Berman) with identical values. The color is green, ranging from bottle green to yellowish green according to the thickness of the plates. The optical properties were determined by immersion in melts by Mr. Bandy and checked by Professor Larsen. Better values, as given below, were obtained by Mr. Berman, using new liquids of unusually high refractive index.

X:*c*-axis = 7° in the acute angle β.	$\alpha = 1.930$		Negative
	$\beta = 2.002$	±0.003	$2V = 71°$
$Z = b$-axis	$\gamma = 2.020$		$r > v$

CHEMICAL COMPOSITION:—A sample of about 1.5 grams was purified by eliminating quartz, as far as possible, with the magnet. The analysis as shown below yields the formula $2CuMoO_4 \cdot Cu(OH)_2$.

ANALYSIS OF LINDGRENITE BY F. A. GONYER

	1	2	3
CuO	40.62	42.8	43.8
MoO_3	50.97	53.7	52.9
H_2O	3.30	3.5	3.3
Fe_2O_3	1.43		
Insoluble (SiO_2)	3.34		
	99.66	100.0	100.0

1. Analysis of lindgrenite. The water was determined on a purer sample than was used for the remaining constituents.
2. Calculated to 100% after removal of 1.43% ferric oxide and 3.34% insoluble (SiO_2) considered as impurities.
3. Theoretical values for $2CuMoO_4$. $Cu(OH)_2$.

The molecular weight of the contents of the unit cell (M) was determined by Mr. Berman from the formula, $M=Vd/A$, where V is the volume of the unit cell (834×10^{-24} c.c.), d is the density (4.26 gm./c.c.), A is the reciprocal of Avogadro's number (1.65×10^{-24}). Whence M is 2154. The following table gives, in terms of oxides, the number of atoms in the unit cell, obtained from M and the found percentage weights of the oxides reduced to 100 per cent.[1]

	Per cent	Mol. ratio	$M\times$mol. ratio/100
CuO	42.8	0.538	11.6
MoO_3	53.7	0.373	8.0
H_2O	3.5	0.194	4.2

Assuming that the numbers in the last column represent the integers 12, 8, 4, respectively,[2] the composition of the unit cell is $12CuO \cdot 8MoO_3 \cdot 4H_2O$, or $4[2CuMoO_4 \cdot Cu(OH)_2]$, or better, $Cu_{12}(MoO_4)_8H_8O_8$, which presupposes no definite arrangement beyond a very probable linking of each atcm of Mo with four atoms of O in the acid radicle.

---

[1] F. A. Bannister and M. H. Hey, *Mineral. Mag.*, vol. **22,** p. 575, 1931.

[2] The differences are due to the combined errors in the determination of the cell dimensions, density and chemical composition.

Lindgrenite is the first molybdate of copper as yet found as a mineral, and neither in form nor in composition can it be grouped with any known natural substance.

Pyrognostics:—Alone on charcoal lindgrenite melts easily, gives a strong reaction for copper when touched with HCl, and reduces to a copper bead. In the closed tube it darkens quickly, decrepitates slightly, giving a slight brownish coating on the wall of the tube near the assay, and melts. There is a fairly abundant deposit of neutral water. It is easily and completely soluble in both HCl and HNO_3; the solution when boiled to dryness and again taken up with acid leaves an abundant heavy white residue of MoO_3, insoluble on boiling; the nature of this residue was first established by a spectrogram for which I am indebted to Dr. G. A. Harcourt.

The author takes great pleasure in designating this well-defined mineral lindgrenite in honor of Professor Waldemar Lindgren. His great contributions to the knowledge of the mineralogy of the ore deposits and their paragenesis makes it peculiarly fitting that his name should appear in the special literature of mineralogy.

THE CRYSTAL STRUCTURE OF SWEDENBORGITE, $NaBe_4SbO_7$

LINUS PAULING, H. P. KLUG, AND A. N. WINCHELL,
Gates Chemical Laboratory, California Institute of Technology.

INTRODUCTION

The hexagonal mineral swedenborgite was first described by Aminoff[1] in 1924 as a sodium aluminum antimonate, with the following properties: colorless to light yellow, hardness about 8, axial ratio $c/a = 1.6309$, definite basal cleavage. Later Aminoff and Blix[2] reported the substance to contain beryllium instead of aluminum, its formula being $NaBe_4SbO_7$. They also suggested several possible atomic arrangements, based on their x-ray examination.

Our interest in the structure of antimonic acid and the antimonates[3] had led us in the meantime to procure specimens of the mineral and begin its study with x-rays. Using the stochastic method,[4] we formulated an atomic arrangement and tested it by a comparison of observed and calculated intensities of reflection. The structure found for swedenborgite, and described in the following pages, is identical with one of those suggested by Aminoff and Blix. Because of the ambiguity of their results, the different nature of our investigation and theirs, and the interesting type of structure found, we believe it worth while to present the following brief account of our work.

We are indebted to Professor Charles Palache of Harvard University for providing us with excellent crystals of swedenborgite, and to Dr. J. Sherman for assistance with the intensity calculations.

THE UNIT OF STRUCTURE AND SPACE GROUP

Data from oscillation photographs of the K radiation of molybdenum led to the values $a_0 = 5.47$ Å and $c_0 = 8.92$ Å for the edges of the hexagonal unit of structure, in approximate agreement with the values of Aminoff and Blix, $a_0 = 5.42$ Å and $c_0 = 8.80$ Å. This unit was found to be compatible with all reflections observed on several completely indexed Laue photographs.

---

[1] G. Aminoff, *Z. Kryst.*, vol. **60**, p. 262, 1924.

[2] G. Aminoff and R. Blix, *Kgl. Sv. Vet. H.*, vol. **11**, p. 3, 1933.

[3] L. Pauling, *Jour. Amer. Chem. Soc.*, vol. **55**, p. 1895, 1933.

[4] See, for example, L. Pauling, *Z. Kryst.* vol. **84**, p. 442, 1933, for a previous application of this method of crystal-structure investigation (to zunyite, $Al_{13}Si_5O_{20}(OH, F)_{18}Cl$).

(The ratio c_0/a_0 agrees with the axial ratio obtained from goniometric measurements. Aminoff reported $c/a=1.6309$, from 36 measurements of the angle $(10\cdot 1)(10\cdot \bar{1})$. We found the value $27°58'17''\pm 12''$ for the angle $(10\cdot 0)(10\cdot 1)$, as the average of 36 measurements; this leads to the axial ratio $c/a=1.6308\pm 0.0003$.)

A Laue photograph prepared with the incident beam parallel to [0001] was found to show a six-fold axis and six planes of symmetry. The point-group symmetry of the crystal is hence D_{3h}, C_{6v}, D_6, or D_{6h}. Of these, C_{6v} is indicated to be correct by Aminoff and Blix's description of one crystal of pronounced hemimorphic face development.

Of the four space groups C_{6v}^1 to C_{6v}^4, two (C_{6v}^2 and C_{6v}^3) are eliminated by numerous observed reflections of the type $(H0\cdot L)$ with L odd. The fact that no reflections of the type $(HH\cdot L)$ with L odd were observed indicates very strongly that the correct space group is C_{6v}^4 (or, if the evidence for hemimorphy is not conclusive, possibly D_{3h}^4 or D_{6h}^4).

FORMULATION OF POSSIBLE ATOMIC ARRANGEMENTS

In formulating possible atomic arrangements we make the following assumptions, based on the rules governing the structure of complex ionic crystals[5] (swedenborgite being considered to contain bonds with sufficient ionic character to make these rules applicable) We shall for convenience use the word ions in referring to the atoms in the crystal, without signifiying that the bonds are all of the extreme ionic type.

1. Each antimony ion is surrounded by six oxygen ions arranged at the corners of an approximately regular octahedron,[3] the antimony-oxygen distance being about 2.0 Å (sum of ionic radii[6] 2.02 Å, sum of covalent radii[7] 2.10 Å).

2. Each beryllium ion is surrounded by four oxygen ions arranged at the corners of an approximately regular tetrahedron, the beryllium-oxygen distance being about 1.65 Å, as in BeO.

3. Each sodium ion is surrounded by six to twelve oxygen ions, at distances greater than 2.35 Å.

4. The electrostatic valence rule is satisfied, each oxygen ion being held by electrostatic bonds with total bond strength 2.

---

[5] L. Pauling, *J. Am. Chem. Soc.*, vol. **51**, p. 1010, 1929.

[6] L. Pauling, *J. Am. Chem. Soc.*, vol. **49**, p. 765, 1927.

[7] L. Pauling and M. L. Huggins, *Z. Kryst.*, vol. **87**, p. 205, 1934. The octahedral radius of antimony, 1.44 Å, is assumed to be 6% greater than the tetrahedral radius.

5. Other factors being equal, the polyhedra will avoid sharing faces and edges.

The strength of a bond from antimony (Sb^{5+}) to each of its six coordinated oxygens (which we shall call O_{II} or O_{III}) is 5/6. The strength of a beryllium bond is $\frac{1}{2}$. Hence each of these oxygen ions is required by the electrostatic valence rule to be common to one antimony octahedron and two beryllium tetrahedra ($5/6+2\times\frac{1}{2}=1\ 5/6$), the remaining 1/6 being made up by sodium bonds.

The seventh oxygen ion of the formula $NaBe_4SbO_7$, which we shall call O_I, is not bonded to antimony. It is accordingly common to four beryllium tetrahedra, thus satisfying the electrostatic valence rule ($4\times\frac{1}{2}=2$).

Our first problem is to construct a suitable framework of octahedra and tetrahedra. We have seen that this will contain groups of four tetrahedra, which have no shared edges. Such a group can be based on a cubic close-packed arrangement of twelve O_{II}'s and O_{III}'s about the central O_I, as illustrated by the group of four tetrahedra shown in Figure 1*a*, or on a hexagonal close-packed arrangement, as shown in Figure 1*b*.

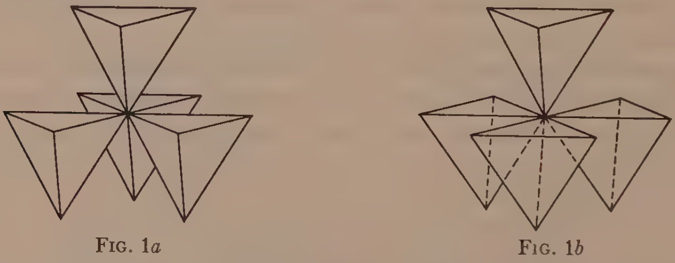
FIG. 1*a* FIG. 1*b*

FIG. 1. Groups of four tetrahedra with a common corner, the twelve outer corners being arranged around the central one (*a*) as in cubic close packing and (*b*) as in hexagonal close packing.

It is seen that the antimony octahedra lie in the same layers as the upper tetrahedra of the groups of four shown in Figure 1; for if they were in the layers below, they would share edges with the tetrahedra. A layer of octahedra at positions required by the value of a_0 is shown in Figure 2. Each of the upper corners of octahedra is to serve as a top corner for an upper tetrahedron. The only way in which this can be achieved is shown in Figure 2*a*. Also each of the lower corners is to serve as top corner for two of the lower tetrahedra. This can be achieved without sharing edges in only one way, shown in Figure 2*b*.

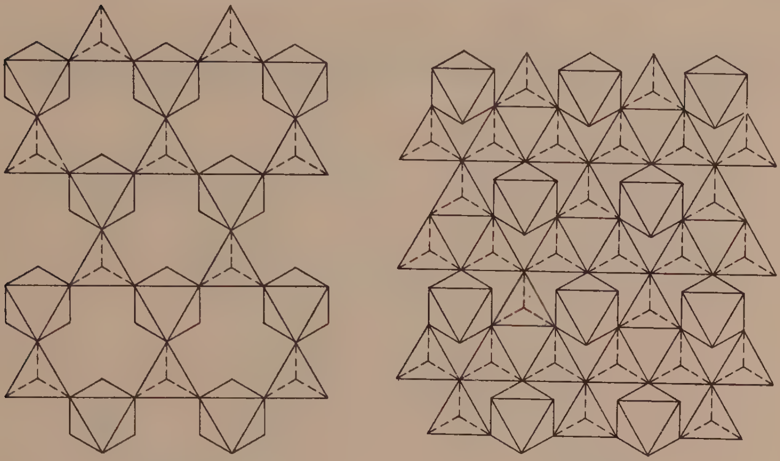

FIG. 2*a* FIG. 2*b*

FIG. 2. Layers of polyhedra in swedenborgite. The same layer of octahedra is shown in 2*a* and 2*b*; in 2*a* the tetrahedra in the same layer are drawn, and in 2*b* the tetrahedra in the layer directly below. It is seen that the groups of four tetrahedra are of the type shown in Figure 1*a*, corresponding to cubic close packing.

We thus have been led to a certain sequence of atom planes, which may be described as follows. Let us designate[8] positions of upper octahedron corners by A, lower corners by C, and octahedron centers by B, using these symbols also for unoccupied close-packed positions. The sequence of atom planes determined above is

$3O_{III}$ at A
  Sb at B, Be_I at C
$1O_I$ and $3O_{II}$ at C
  3 Be_{II} at B
$3O_{III}$ at B.

It is seen that oxygen atoms O_I and O_{II} are surrounded by other oxygen atoms in the way corresponding to cubic close packing.

In addition, we know that the upper octahedron corners are to serve as lower corners for the next higher layer of tetrahedra. However, this does not fix the positions of these tetrahedra, for their upper corners can occupy either positions C or positions B, the first alternative corresponding to hexagonal close-packing of oxygen atoms about O_{III} and the second to cubic close-packing.

---

[8] This convenient nomenclature for close-packed layers can be defined by the use of hexagonal coordinates in a plane as follows: A, $X=0$, $Y=0$; B, $X=1/3$, $Y=2/3$, and C, $X=2/3$, $Y=1/3$.

Corresponding to these alternatives we obtain two distinct but very closely related structures, represented by the following schemes.

	HEXAGONAL STRUCTURE				CUBIC STRUCTURE				
	Na, 3 $\mathrm{O_{III}}$ at *A*				Na, 3 $\mathrm{O_{III}}$ at *A*				
↑		Sb at *B*, $\mathrm{Be_{I}}$ at *C*				Sb at *B*, $\mathrm{Be_{I}}$ at *C*			↑
	$\mathrm{O_{I}}$, 3 $\mathrm{O_{II}}$ at *C*				$\mathrm{O_{I}}$, 3 $\mathrm{O_{II}}$ at *C*				
		3 $\mathrm{Be_{II}}$ at *B*				3 $\mathrm{Be_{II}}$ at *B*			
c_0	Na, 3 $\mathrm{O_{III}}$ at *B*				Na, 3 $\mathrm{O_{III}}$ at *B*				
		A		*C*		*C*		*A*	
	C				*A*				
			A				*C*		c_0
	A				*C*				
↓		*B*		*C*		*A*		*B*	
	C				*B*				
			B				*A*		
	B				*A*				
	etc.					*B*		*C*	↓
					C	etc.			

The first of these structures repeats after two layers, and so leads to a unit of the size observed for swedenborgite. It is the structure of swedenborgite. This structure is based on double hexagonal close-packing of oxygen ions, first found in brookite[9] and topaz.[10] Of the sixteen close-packed positions in the unit, only fourteen are occupied by oxygens; we place sodium ions in the other two, thus giving sodium the coordination number 12. The structure has the symmetry of space group C_{6v}^4, and the predicted values of a_0 and c_0 (based on the assumed interatomic distances) agree perfectly with the observed values. These facts, together with the agreement with general structural principles, provide strong support for the structure. Further verification is given by the agreement of observed and calculated *x*-ray intensities, discussed in the following section.

The second structure repeats after three layers, and, indeed, has cubic symmetry rather than hexagonal symmetry. From the standpoint of crystal chemistry this structure is not inferior to the other for the compound $\mathrm{NaBe_4SbO_7}$, and we predict that cubic crystals of this substance may be discovered, for which the face-centered unit of structure, containing 4 $\mathrm{NaBe_4SbO_7}$, will have $a_0 = 7.72$ Å.

---

[9] L. Pauling and J. H. Sturdivant, *Z. Kryst.*, vol. **68**, p. 239, 1928.

[10] L. Pauling, *Proc. Nat. Acad. Sci.*, vol. **14**, p. 603, 1928.

VERIFICATION OF THE STRUCTURE

In terms of the equivalent positions of space group C_{6v}^4,

$2a$: $0 0 u$, $0 0 \frac{1}{2}+u$;
$2b$: $\frac{1}{3}\ \frac{2}{3} u$, $\frac{2}{3}\ \frac{1}{3}\ \frac{1}{2}+u$;
$6c$: $u\ \bar{u}\ v$, $2\bar{u}\ \bar{u}\ v$, $u\ 2u\ v$,
$\bar{u}\ u\ \frac{1}{2}+v$, $2u\ u\ \frac{1}{2}+v$, $\bar{u}\ 2\bar{u}\ \frac{1}{2}+v$;

the ideal atomic arrangement (for regular polyhedra) can be described as follows:

2 Sb at $2b$, $u=0$;
2 Na at $2b$, $u=\frac{5}{8}$;
2 Be_{I} at $2a$, $u=\frac{1}{16}$;
2 O_{I} at $2a$, $u=\frac{3}{8}$;
6 Be_{II} at $6c$, $u=\frac{1}{6}$, $v=\frac{5}{16}$;
6 O_{II} at $6c$, $u=\frac{1}{2}$, $v=\frac{3}{8}$;
6 O_{III} at $6c$, $u=\frac{1}{6}$, $v=\frac{1}{8}$.

We have calculated intensities of reflection for a large number of planes on the basis of this arrangement, using the customary bath-method formula

$$I_{HI\cdot L}=\text{Constant}\cdot\frac{1+\cos^2 2\theta}{2\sin 2\theta}\,|F_{HI\cdot L}|^2,$$

$$\text{with } F_{HI\cdot L}=\sum f_j e^{2\pi i}(Hx_j+Iy_j+Lz_j)$$

the sum being taken over all atoms in the unit. Pauling-Sherman f-values[11] were used, and the temperature factor omitted, the error due to this omission being small for such a hard crystal. The results of the calculation are given in Table 1, for comparison with the observed intensity values on oscillation photographs. The photographs were made with the K-radiation of molybdenum filtered through zirconia, with 30° oscillation about $[1\bar{1}\cdot 0]$ through various angular regions. Estimates of intensity values were made by the visual comparison of films prepared under identical conditions except for changed time of exposure. The Ott correction was made for reflections not in the equator.

It is seen that the agreement is satisfactory, providing strong evidence that the suggested structure is correct. Further evidence is given by the fact that the ideal arrangement requires that no reflections of the type $\frac{H+2I}{3}$ integral, L odd occur. None such was observed on the photographs.[12]

---

[11] L. Pauling and J. Sherman, *Z. Kryst.*, vol. **81**, p. 1, 1932.

[12] Several reflections apparently of this type were observed on one series of photographs; it was then found that these were due to reflections from a twinned crystal We have not determined the type of twinning involved.

The number of parameters is so great that it is not practicable to attempt to determine deviations from the ideal values.

Our intensity data agree with those of Aminoff and Blix, so far as they overlap. Our structure is identical with one of those suggested by them, and found by them to be compatible with their data.

TABLE 1

CALCULATED AND OBSERVED INTENSITIES OF X-RAY REFLECTION FOR SWEDENBORGITE

	Intensity			*Intensity*	
HI·L	Calculated	Observed	HI·L	Calculated	Observed
11·0	50	50	20·2	20	36
22·0	52	45	30·2	15	18
33·0	4.8	5	40·2	3.5	3.5
44·0	8.0	6	50·2	1.1	2
55·0	1.5	2	60·2	2.5	4
22·2	7.8	10	21·0	5.1	5
33·2	4.9	5	21·2	4.1	4
44·2	1.8	2.5	31·0	2.5	3
55·2	1.6	3	31·1	6.0	10
33·4	3.2	5	31·2	2.0	3
44·4	0.4	0.5	31·3	7.6	10
55·4	1.3	2	32·1	4.0	6
33·6	2.5	4	32·2	1.4	2
44·6	2.2	2	32·3	5.3	7
55·6	1.1	2	32·4	0.5	2
44·8	2.9	3	41·2	6.6	9
55·8	1.2	2	41·4	3.6	5
44·10	1.7	1	42·1	3.4	3
40·1	5.4	8	42·2	1.5	2
50·1	5.6	7	42·3	2.1	4
40·3	8.3	8	42·4	1.0	1.5
50·3	1.8	5	42·5	3.8	5.0
50·5	2.1	4	42·6	2.2	2
10·0	16.0	23	42·7	1.7	1
20·0	2.6	4.5	43·4	0.6	1
30·0	17.1	18.0	43·5	1.8	2
40·0	0.9	0	43·6	0.6	0.5
50·0	0.9	0	43·7	1.5	1.5
			43·8	0.8	0.5

Their other structures are of types which we eliminated early in our process of formulating a structure because of conflict with the assumed structural characteristics.

DESCRIPTION OF THE STRUCTURE

The structure of swedenborgite is shown in Figure 3. Its general nature has been discussed in the process of its formulation.

Each beryllium ion is surrounded by four oxygen ions at tetrahedron corners, the Be-O distance (for ideal parameter values) being 1.67 Å. Each antimony ion is surrounded by six oxygen ions at octahedron corners. It seems probable, in view of the predicted values 2.02–2.10 Å for the Sb-O distance, that there is some distortion of the structure, increasing the Sb-O distance somewhat above the value 1.93 Å corresponding to the ideal parameter values, and decreasing the Be-O distance to about 1.65 Å, as in beryllium oxide.

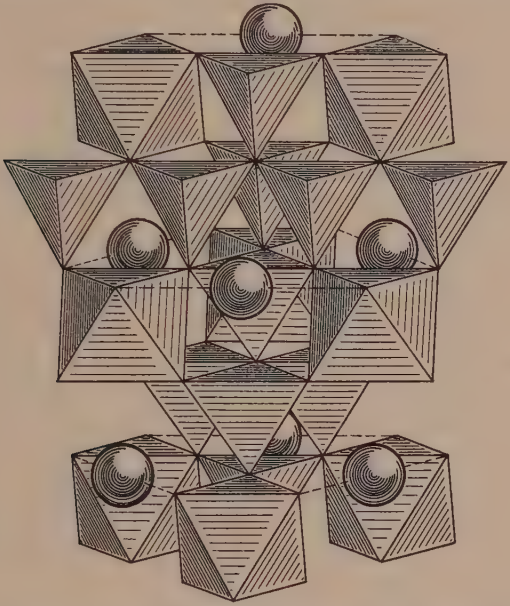

FIG. 3. A portion of the structure of swedenborgite, showing the antimony octahedra, the groups of four beryllium tetrahedra, and the sodium ions (represented by spheres). The oxygen and sodium ions together form a double hexagonal close-packed aggregate.

Each sodium ion is surrounded by twelve oxygen ions at about 2.7 Å, a value compatible with the radius sum 2.35 Å in view of the large coordination number.

Each O_I is reached by four beryllium bonds, of strength $\frac{1}{2}$, and each O_{II} and O_{III} by one antimony bond (5/6), two beryllium bonds

($\frac{1}{2}$), and two sodium bonds (1/12), the electrostatic valence rule thus being exactly satisfied.

The crystal provides an excellent type of structure for a complex ionic substance, illustrating most of the general rules for such structures, as discussed in an earlier section. The substance can be considered as a basic antimonate (salt of the acid H_7SbO_6) of sodium and beryllium. It bears an interesting relation to basic beryllium acetate,[13] $Be_4O(CH_3COO)_6$; in the molecules of this substance there occur four beryllium tetrahedra with one common corner, the twelve remaining corners being occupied by carboxyl oxygens, whereas in swedenborgite these twelve corners are occupied by oxygen atoms common to two tetrahedra (in different groups) and one antimonate octahedron. The chemical formula of swedenborgite might well be written as $NaBe_4OSbO_6$.

The vertical columns of tetrahedra (one of which is shown in Figure 3) form an interesting feature of the structure. It might be expected that these would cause the crystal to show prismatic cleavage. A simple consideration[14] of the number of bonds broken by cleavage along various planes shows, however, that basal cleavage is to be expected, in agreement with observation. The very strong antimony bonds will resist rupture, and the sodium bonds can be neglected. Cleavage along (00·1) requires three beryllium bonds to be broken per unit rhomb, with area $\sqrt{3}a_0^2/2 = 25.8$ Å², or 0.116 bond per Å², whereas for (10·0) there are four bonds per 24.4 Å² or 0.164 per Å², and for (11·0) eight bonds per 42.3 Å² or 0.189 per Å².

Summary

The hexagonal unit of swedenborgite, containing $2NaBe_4SbO_7$, has $a_0 = 5.47$ Å and $c_0 = 8.92$ Å. The atomic arrangement, in terms of the equivalent positions of space group C_{6v}^4, is the following:

2 Sb at $2b$, $u=0$;
2 Na at $2b$, $u=\frac{5}{8}$;
2 Be_I at $2a$, $u=\frac{1}{16}$;
2 O_I at $2a$, $u=\frac{3}{8}$;
6 Be_{II} at $6c$, $u=\frac{1}{6}$, $v=\frac{5}{16}$;
6 O_{II} at $6c$, $u=\frac{1}{2}$, $v=\frac{3}{8}$;
6 O_{III} at $6c$, $u=\frac{1}{6}$, $v=\frac{1}{8}$.

---

[13] L. Pauling and J. Sherman, *Proc. Nat. Acad. Sci.*, vol. **20**, p. 340, 1934.

[14] For the similar discussion of cleavage of aluminosilicate crystals see L. Pauling, *Proc. Nat. Acad. Sci.*, vol. **16**, p. 453, 1930, and M. D. Shappell, *Dissertation*, California Institute of Technology, 1933.

The crystal contains octahedral SbO_6 groups, and groups of four beryllium tetrahedra with one corner common to all four, the other corners being shared with tetrahedra of other groups and with antimony octahedra. The large oxygen and sodium ions are arranged in double hexagonal close packing.

EVOLUTION OF THE WHITE MOUNTAIN MAGMA SERIES

Randolph W. Chapman, *Vassar College*
and
Charles R. Williams, *Cambridge, Mass.*

PART I. DATA

Problem

In recent years, a number of intensive field and laboratory studies of the rocks of the White Mountain district in New Hampshire have been carried out. One result of these investigations is to show that there exists in this area a group of rocks with marked alkaline affinities (3)* to which the name White Mountain magma series has been applied (5, p. 56). The various rock types of this group form a definite series, and wherever found in the area they possess the same relative ages. Such a sequence is of greatest importance to petrology and necessitates an explanation. Accordingly, the writers have undertaken a study of this problem, the results of which are presented in this paper. It is not pretended that this work is complete or that the problem has been entirely solved. Certain definite conclusions have been reached, however, and it is hoped that these may lead to a more complete understanding of the evolution of the White Mountain magma series.

The writers are especially indebted to Professor Marland Billings of Harvard University for his valuable assistance in preparing this paper. Several of the major ideas presented here were first suggested by Professor Billings, and these have led to a clearer understanding of many of the intricate problems encountered in the course of the work. The writers also wish to thank Professor Esper S. Larsen, Jr., and Professor R. A. Daly for their many helpful suggestions and criticisms. The new mineral analyses quoted here were made by F. A. Gonyer of Harvard University.

In the course of these investigations the writers have limited themselves entirely to those areas with which they are personally familiar, either from a field study or from a study of rock collections. These areas include the North Conway quadrangle, the Ossipee Mountains, the Belknap Mountains, Pleasant Mountain in Maine, the Franconia quadrangle, the Percy quadrangle, Tripyramid Mountain, and Red Hill. The rock types of each of these

---

* Numbers in parentheses refer to bibliography at end of paper.

Table 1. Data on the Plutonic Rocks of the White Mountain Magma Series

NAME	GABBRO	NORITE	DIORITE	QUARTZ DIORITE	MONZODIORITE	MONZONITE	NEPHELITE SYENITE	ANALCITE SYENITE
DISTRIBUTION	TRIPYRAMID MTN. BELKNAP MTNS.	TRIPYRAMID MTN.	NORTH CONWAY QUAD. PLEASANT MTN. FRANCONIA REGION	FRANCONIA REGION	BELKNAP MTNS.	TRIPYRAMID MTN. PLEASANT MTN.	RED HILL	PLEASANT MTN.
SIZE OF BODIES	FEW SQ.FT. TO 0.25 SQ. MI.	NOT KNOWN	FEW SQ.FT. TO 0.2 SQ.MI.	1.5 SQ. MI.	0.25 TO 2 SQ. MI.	RING-DIKE - 2.5 MI. DIAMETER SMALL MASS - 0.01 SQ. MI.	NOT KNOWN	0.03 SQ. MI.
SHAPE OF BODIES	IRREGULAR	NOT KNOWN	SMALL STOCKS AND DIKES	ROUGHLY CIRCULAR	INCOMPLETE RING-DIKES	IRREGULAR AND RING-DIKE	NOT KNOWN	SMALL PERIPHERAL BAND ON MAIN STOCK
TOTAL AREA AND PER CENT OF MAGMA SERIES	0.10 SQ. MI. 0.02 %	VERY SMALL	0.25 SQ. MI. 0.055 %	1.5 SQ.MI. 0.33 %	4.0 SQ. MI. 0.87 %	2.6 SQ. MI. 0.57 %	VERY SMALL	0.03 SQ MI. 0 007 %
TEXTURE	HYPIDIOMORPHIC, GRANULAR BELKNAPS - DIABASIC	HYPIDIOMORPHIC, INEQUIGRANULAR	HYPIDIOMORPHIC, INEQUIGRANULAR	HYPIDIOMORPHIC, INEQUIGRANULAR	HYPIDIOMORPHIC, EQUIGRANULAR TO SUBPORPHYRITIC	HYPIDIOMORPHIC, INEQUIGRANULAR	HYPIDIOMORPHIC, GRANULAR	ALLOTRIOMORPHIC, INEQUIGRANULAR
DIAMETER OF GRAINS	5 - 10 MM.	1 - 3 MM.	1 - 4 MM.	2 - 3 MM.	DARK MINERALS - 0.5 MM. REST 2 - 5 MM.	1 - 5 MM.	2 - 5 MM. AVG. 2 - 3 MM.	0.5 - 5 MM.
COLOR	DARK GRAY TO BLACK	DARK MOTTLED	DARK MOTTLED	LIGHT GRAY MOTTLED	LIGHT GRAY	GRAY	LIGHT GRAY	LIGHT GRAY
MODE	TRIPY. BEL. LAB. 63.0 49.0 HBD. — 22.0 AUG. 14.0 18.0 IL. 6.7 5.0 BI. 5.0 — OL. 10.0 — OR. .5 — ACC. 0.8 6.0 100.0 100.0 ACC. - PY. TI. AP. CHL. HY	QTZ. 3.0 LAB. 56.5 OR. 3.0 HY. 10.0 DI. 5.6 BI. 6.0 AP. 4.4 MT. 11.0 ACC. 0.5 100.0	P.M. F. AND. 62.0 65.0 BI. 17.5 12.0 AUG. 15.5 8.0 AP. 1.5 TR. MT. 4.0 TR TI. TR. TR. CHL. — 14.0 ACC. — 1.0 100.5 100 0 ACC.- HBD. PY. QTZ	AND. 63.0 OR. 2.0 BI 15.0 HBD. 9.0 QTZ. 10.0 ACC. 1.0 100.0 ACC. - AP MT	I II III AND. — — 72.0 OLIG. 61.0 61.0 — OR. 21.0 20.0 12.0 AUG. 7.0 5.0 — BI. 4.0 10.0 3.0 HBD. 3.0 2.0 7.0 QTZ. 2.0 — 4.0 ACC 2.0 2.0 2.0 100.0 100.0 100.0 ACC.- DI AP MT. ZR. CHL.	TRIPY. P.M. AND. 40.0 47.0 MP. — 40.0 OR. 40.0 — HBD. 12.0 — DI. 3.0 — AUG. — 1.5 BI. — 8.0 ACC. 5.0 3.0 100.0 99.5 ACC.- AP IL. MT TI ALL.	OR. 36.0 AB. 37.0 NEPH. 14.0 SOD. 5.0 HBD. 7.0 ACC. 1.0 100.0 ACC.- AP. ZR. DI. BI. AEG MT. CANCRINITE WOHLERITE	I II III MP. 80.5 82.0 84 0 OLIG. 3.5 2.5 — ANAL. 6.5 6.5 7.5 HBD. 7.5 5.5 4 5 TI. 2.5 2.5 1 5 MT. 0.6 0.5 1 5 AP. TR. 0.7 TR ZR. TR. TR. TR. 100.6 100.2 99 0

CHEMICAL COMPOSITION	GABBRO TRIPY.	GABBRO BEL.	NORITE	DIORITE	QUARTZ DIORITE	MONZODIORITE MODE I	MONZONITE	NEPHELITE SYENITE	ANALCITE SYENITE MODE I
SiO_2	48.04	43.94	48.67			56.66		58.30	60.96
TiO_2	2.56	4.13	2.12			1.55		.10	60
Al_2O_3	20.10	16.17	16.88			19.03		21.38	19 20
Fe_2O_3	2.32	3.96	4.98			2.67		1 05	1.24
FeO	6.13	10.06	6.37			4.88		2.04	1.63
MnO	.09	—	—			—		TR.	18
MgO	4.68	5.05	4.62			1.86		.22	.55
CaO	11.52	9.59	8.63			4.82		.95	1.86
Na_2O	3.01	2.93	3.85			4.52		8.66	7.07
K_2O	79	1.51	1.26			3 62		6.06	5.54
H_2O^+	.42	1.42	.32			60		.45	58
H_2O^-	—	13	.02					35	04
ZrO_2	ND	ND	ND			ND		02	07
P_2O_5	.15	.69	1.85			ND		.04	14
Cl	ND	CO_2 .09	ND			ND		.35	BaO .06
S	08	ND	ND			07		08	ND
TOTALS	100.06	99.67	99.57			100.37		100.05	99.80

ABBREVIATIONS

AB - ALBITE
ACC - ACCESSORIES
AEG - AEGIRINE
ALL - ALLANITE
ANAL - ANALCITE
AND - ANDESINE
AP - APATITE
AST - ASTROPHYLLITE
AUG - AUGITE
BI - BIOTITE
CHL - CHLORITE
DI - DIOPSIDE
FAY - FAYALITE
FL - FLUORITE
HAST - HASTINGSITE
HBD - HORNBLENDE
HED - HEDENBERGITE
HY - HYPERSTHENE
IL - ILMENITE
LAB - LABRADORITE
MP - MICROPERTHITE
MT - MAGNETITE MAY INCLUDE IL
NEPH - NEPHELINE
OL - OLIVINE
OLIG - OLIGOCLASE
OR - ORTHOCLASE
PY - PYRITE
PYROX - PYROXENE
QTZ - QUARTZ
RIEB - RIEBECKITE
SOD - SODALITE
TI - TITANITE
ZR - ZIRCON

NAME	SYENITE	QUARTZ SYENITE	QUARTZ SYENITE ALBANY TYPE	GRANITE PORPHYRY	HASTINGSITE GRANITE	RIEBECKITE GRANITE	BIOTITE GRANITE
DISTRIBUTION	NORTH CONWAY BELKNAP MTNS. PLEASANT MTN. TRIPYRAMID MTN. FRANCONIA REG. RED HILL PERCY QUAD.	NORTH CONWAY BELKNAP MTNS.	NORTH CONWAY QUAD. BELKNAP MTNS. OSSIPEE MTNS. FRANCONIA REGION	FRANCONIA REGION	NORTH CONWAY QUAD. PERCY QUAD.	NORTH CONWAY QUAD. PERCY QUAD.	NORTH CONWAY QUAD. OSSIPEE MTNS. BELKNAP MTNS. PERCY QUAD. FRANCONIA REGION TRIPYRAMID
SIZE OF BODIES	0.10 - 20.0 SQ. MI.	1.5 - 6.0 SQ.MI.	WIDTH - 0.25 - 1.5 MI. DIAMETER - 8 - 9 MI.	WIDTH 1 - 3 MI. 43.2 SQ. MI.	STOCKS - 1.5 TO 4.0 MILES IN DIAMETER. RING-DIKES - WIDTH 0.25 - 1.0 MI. LENGTH 1 - 4 MI.		STOCKS: 1 - 5 MI. IN DIAMETER A FEW SMALL RING-DIKES
SHAPE OF BODIES	RING-DIKES AND IRREGULAR STOCKS		RING-DIKES	IRREGULAR RING-DIKE	N.C. - IRREGULAR P - INCOMPLETE RING-DIKES	N.C. - SMALL IRREG. BODIES P.- INCOMPLETE RING-DIKES	LARGE STOCKS OF IRREGULAR SHAPE. AND VARYING SIZE. A FEW SMALL RING-DIKES.
TOTAL AREA AND PER CENT OF MAGMA SERIES	43.1 SQ. MI. 9.41 %	7.5 SQ. MI 1.64 %	39.9 SQ. MI 8.71 %	43.2 SQ. MI 9.43 %	ALL GRANITES 315.5 SQ. MI. 68.9 %		
TEXTURE	HYPIDIOMORPHIC, GRANULAR. SOME PORPHYRITIC SOME TRACHYTIC		PORPHYRITIC, GROUND MASS PANALLOTRIOMORPHIC TO HYPIDIOMORPHIC GRANULAR	PORPHYRITIC, GROUND MASS PANALLOTRIOMORPHIC	HYPIDIOMORPHIC, GRANULAR	HYPIDIOMORPHIC, GRANULAR TO MICROPEGMATITIC	HYPIDIOMORPHIC, GRANULAR. SOME PHASES PORPHYRITIC
GRAIN SIZE	0.5 - 5.0 MM.		DARK MINERALS: 0.5 - 1.2 MM. REST: 1.0 - 8.0 MM.	GROUND MASS: 0.06 - 0.3 MM. PHENOCRYSTS: 5.0 - 8.0 MM. DARK MINERALS: 0.6 - 1.4 MM.	0.5 - 3.0 MM.	0.5 - 3.0 MM.	0.5 - 10.0 MM. PHENOCRYSTS OFTEN UP TO 1.5 CM.
COLOR	GRAY. GREEN. BLUISH		DARK GRAY. GREEN OR PINK	DARK GRAY AND PINK	LIGHT GRAY TO WHITE	SNOWY WHITE. MOTTLED	PINK TO GREEN. SPOTTED WITH DARK MINERALS
MODE	BEL. PERCY P.M. TRIPY QTZ. — 1.6 3.0 1.0 OR 47.0 — — — MP — 86.6 83.0 80.0 OLIG 42.0 — 7.0 — LAB — — — 6.5 BI 2.0 — 1.5 1.0 HBD 7.0 3.2 TR 6.0 HED — 3.4 — — PYROX — — 1.5 1.0 FAY — 1.9 — — ACC 2.0 2.9 3.3 4.5 100.0 99.6 99.3 100.0	BEL. N.C. QTZ 8.0 6.3 OR 40.0 } 75.9 OLIG 39.0 BI 2.0 0.4 HBD 7.0 — HAST — 12.6 HED — 3.6 ACC 2.0 1.2 100.0 100.0	N.C. BEL. F QTZ 12.6 15 0 13.8 MP } 74.1 59.1 OR 71.0 17 1 OLIG 12.0 2.7 HAST 12.3 12.0 3.8 HED — — 2.4 FAY — — 0.6 BI 0.5 — — ACC 0.5 2.0 0.5 100.0 100.0 100.0 ACC: MT. AP. ZR. AL. FL	AVG. MODE QTZ 26.5 MP 23.5 OR 34 9 OLIG 1 4 HAST 6 1 HED 5.1 FAY 1.0 BI 1.2 ACC 0.6 100.0 ACC: FL. ALL. AP. ZR. MT	N.C. PERCY QTZ 17 4 24.0 MP } 72.6 66.5 OLIG 0.5 HAST 8.3 8.0 HED — 0.4 BI 0.6 — ACC 1.1 0.6 100.0 100.0 ACC: AL. AP. ZR. FL. MT. AEG	N.C. PERCY QTZ 39.4 38.5 MP } 54.0 53.8 OLIG 0.7 RIEB 5.5 5.8 BI — 0.7 AST 1.1 — ACC — 0.5 100.0 100.0 ACC: ZR. MT. IL. TI. AP FL	N.C. BEL. PERCY F. QTZ 26.7 30.0 23.0 39.0 34.2 35.1 25.9 26.5 MP — — 44.4 39.2 55.3 } 69.8 OR } 69.4 68.4 37.0 } 56.0 — — — — OLIG 34.0 16.6 21.9 15.3 BI 3.0 1.6 } 4.0 3.0 4.2 2.8 2.9 1.4 HAST 0.2 — — — — — 1.6 ACC 0.7 — 2.0 2.0 0.1 0.9 0.6 0.6 100.0 100.0 100.0 100.0 100.0 100.0 100.0 100.0 ACC: FL. ALL. MT. IL. AP HBD

CHEMICAL COMPOSITION	SYENITE BEL.	SYENITE TRIPY.	SYENITE P.M.	QUARTZ SYENITE N.C.	QUARTZ SYENITE ALBANY TYPE N.C.	QUARTZ SYENITE ALBANY TYPE BEL.	GRANITE PORPHYRY	HASTINGSITE GRANITE	RIEBECKITE GRANITE	BIOTITE GRANITE NORTH CONWAY RED PHASE	BIOTITE GRANITE NORTH CONWAY BALDFACE PHASE	BIOTITE GRANITE NORTH CONWAY BLACK CAP PHASE	BIOTITE GRANITE NORTH CONWAY RED PHASE
SiO_2	60.75	62.12	63.32	62.24	64.40	66.14	71 88			70.45	73.65	72 35	73.01
TiO_2	0.63	0.84	0.52	0.87	0.88	0.51	0.25			0.69	0.22	0.39	ND
Al_2O_3	19.55	15.57	18.75	15.82	16.75	17.04	13.64			14.87	13.73	12.48	13.73
Fe_2O_3	1.54	2.16	1.24	1.94	1.3	1.24	1 36			1.07	0 23	1.22	0.44
FeO	2.98	2.59	1.77	4.69	3.44	2.10	1.99			1.54	0.95	1.25	1.48
MnO	ND	TR	0.11	0.24	0.05	—	0.03			—	TR	0.03	0.09
MgO	0.81	0.86	0.71	0.07	0.62	0.21	0.17			0.35	0.11	0.42	0.01
CaO	2.29	2.37	2.03	2.65	1.85	1.62	0.90			1.28	0.90	1.19	0.94
Na_2O	4.89	6.78	6.04	4.80	4.44	4.88	3.73			4.28	4.47	3.76	3.50
K_2O	5.90	4.79	4.88	6.26	4.96	5.54	5.61			4.16	4.27	5.98	5.62
H_2O^+	0.08	0.48	0.36	0.56	1.05	0.41	0.29			0.65	0.77	0.80	0.18
H_2O^-	0.24	0.09	0.06	0.07	0.22	—	—			0.50	0.56	0.17	0.05
ZrO_2	ND	ND	0.05	ND	ND	ND	ND			ND	ND	ND	ND
P_2O_5	0.13	0.23	0.16	0.14	0.11	0.08	TR			0.04	TR	0.27	ND
Cl	ND	ND	SrO 0.03	ND	ND	ND	ND			ND	ND	ND	ND
S	ND	ND	BaO 0.11	ND	ND	ND	0.02			ND	ND	ND	ND
TOTALS	99.79	100.88	100.24	100.35	100.08	100.08	99.87			99.88	99.86	100.11	99.05

regions is shown in some detail in Figure 1. It is entirely possible, and in fact likely, that such areas as Mount Ascutney in Vermont, the Burnt Meadow Mountains in Maine, and the Pawtuckaway Mountains of New Hampshire also contain rocks belonging to this magma series, but due to the fact that they have not been studied by the present investigators, they will not be considered in this discussion.

Briefly, the method of attack consisted of both field and laboratory studies. The field studies served to determine the sizes of rock bodies and the age relations of the various rock types of the series. In the laboratory the mineralogy and chemistry of the rocks, and the optics and chemistry of the minerals were determined. Particular emphasis was given to the evolution of the mineral species, for the writers feel that such a method of attack must be adopted if problems in the evolution of igneous rocks are to be solved.

ROCKS

PETROGRAPHY AND CHEMISTRY. The rocks of the White Mountain magma series may be classified into three main groups: volcanic rocks, plutonic rocks, and dike rocks. The volcanic rocks consist of flows, tuffs, and breccias of basalt, andesite, trachyte, and rhyolite. The plutonic rocks are gabbro, norite, diorite, quartz diorite, monzodiorite, monzonite, nephelite syenite, analcite syenite, syenite, quartz syenite, quartz syenite (Albany type), granite porphyry, hastingsite granite, riebeckite granite, and biotite granite. The dike rocks are listed below. The distribution of the volcanic and plutonic rocks is shown in Figure 1. For the sake of simplicity, all the granites have been indicated with one pattern, and the monzodiorites and monzonites with another pattern. All the other rocks have been mapped with separate patterns. The data have been obtained from the published works of Billings (3), Kingsley (26), Jenks (23), Pirsson and Rice (33), Pirsson and Washington (31 and 32), and the unpublished works of Modell (28), Williams (40), Chapman (9), Billings (6), and Page (29). Mount Monadnock, Vermont, and a number of bodies in which the different rock species have not been distinguished are shown on the map, but they were not considered in the present study. Since the map was prepared, Dr. A. W. Quinn of Brown University has completed a study of Red Hill.

Lack of space prohibits a complete description of each rock type;

accordingly, most of the data have been listed in tabular form. Table 1, which is self-explanatory, gives the most important characteristics of the plutonic phases, together with their modes and chemical analyses. The rocks are listed according to age as nearly as possible, except that the quartz syenite (Albany type) has been placed before the granite porphyry. This was done so that the quartz syenite and the quartz syenite (Albany type) might be compared more easily. Many of the data are new and are published here for the first time. Those for the Belknaps, Percy, and Franconia regions are from the unpublished works of Modell, Chapman, and Williams respectively. The following chemical analyses are also new: gabbro from Tripyramid Mountain, monzodiorite from the Belknaps, Albany quartz syenite from the Belknaps, and granite porphyry from the Franconia quadrangle.

The chief characteristics of the volcanic rocks, which cover about 30 square miles, are shown in Table 2. The dikes belonging to the magma series are very abundant and consist of olivine diabase, kersantite, diorite, camptonite, spessartite, augite syenite porphyry, porphyritic syenite, syenite porphyry, bostonite, hastingsite sölvsbergite, paisanite, hastingsite granite, biotite granite, aplite, and quartz porphyry. A list of their chemical analyses is given in Table 3.

TABLE 2

VOLCANIC ROCKS OF THE WHITE MOUNTAIN MAGMA SERIES*

NAME	*Basalt*	*Andesite*	*Trachyte*	*Rhyolite*
DISTRIBUTION	Ossipee Mtns.	Ossipee Mtns. Franconia Quad.	North Conway Pleasant Mtn. Belknap Mtns.	North Conway Ossipee Mtns. Belknap Mtns. Franconia Quad.
TEXTURE	Porphyritic	Trachytic and porphyritic	Trachytic and porphyritic	Porphyritic
GRAIN SIZE	Dense groundmass	Dense groundmass	Dense groundmass	Dense groundmass
COLOR	Black	Black	Gray, black, red, purple	Red, gray, yellow, brown, pink
MINERALS	Labradorite Augite-diopside Amphibole	Andesine Alkali feldspar Amphibole	Orthoclase Oligoclase Albite	Microperthite Soda-orthoclase Albite

Table 2 (*Continued*)

Magnetite	Apatite	Soda-orthoclase	Oligoclase
Titanite	Magnetite	Microperthite	Quartz
Pyrite	Epidote	Quartz	Hastingsite
Epidote	Chlorite	Zircon	Biotite
Calcite	Sericite	Magnetite	Fayalite
Chlorite	Leucoxene	Biotite	Fluorite
		Apatite	Zircon
		Clinozoisite	Magnetite
		Augite	Riebeckite
		Hornblende	Aegirine-augite
		Titanite	Hornblende
		Epidote	Apatite
		Chlorite	Titanite
			Allanite
			Chlorite
			Epidote

Chemical Analyses of Volcanic Rocks of White Mountain Magma Series

	1	2	3	4	5	6	7
SiO_2	49.04	57.85	65.05	75.38	73.33	72.25	72.05
TiO_2	3.74	2.34	.25	nd	nd	nd	.23
Al_2O_3	18.10	16.30	16.80	11.85	12.95	13.40	14.72
Fe_2O_3	2.31	3.16	4.97	1.78	.98	1.10	1.02
FeO	6.69	5.10	1.12	.88	1.66	1.53	1.46
MnO	.08	.10	tr	.10	1.13	.11	tr
MgO	3.68	2.68	.20	none	none	none	.15
CaO	10.72	5.50	1.68	.33	.98	.74	.79
Na_2O	2.53	3.00	3.94	3.68	3.46	4.27	4.42
K_2O	1.09	2.92	5.22	5.37	5.61	5.56	4.00
H_2O+	1.72	.61	.30	.50	.30	.31	.55
H_2O-	.12	.10	.45	.15	.11	.10	.55
P_2O_5	.08	.13	tr	nd	nd	nd	nd
Totals	99.90	99.80	99.98	100.02	99.51	99.37	99.94

1. Basalt—Bald Knob, Ossipee Mountains (26, p. 159).
2. Andesite—Cold Brook, Ossipee Mountains (26, p. 159).
3. Trachyte—South Moat Mountain, North Conway quadrangle (3, p. 97).
4. Quartz porphyry—south slope Mt. Pequawket, North Conway quadrangle (30, p. 408).
5. Quartz porphyry—east slope Mt. Pequawket, North Conway quadrangle (30, p. 409).
6. Quartz porphyry—summit Mt. Pequawket, North Conway quadrangle (30, p. 409).
7. Riebeckite quartz porphyry—Dry Brook, Albany, North Conway quadrangle (3, p. 95).

* These rocks occur in part as tuffs and breccias.

TABLE 3

CHEMICAL ANALYSES OF DIKE ROCKS OF WHITE MOUNTAIN MAGMA SERIES

	1	2	3	4	5	6	7	8	9	10
SiO_2	69.51	50.75	50.59	76.65	52.95	42.73	41.63	42.77	41.94	58.25
TiO_2	.29	3.05	2.60	.05	3.90	4.30	3.95	2.35	4.15	tr
Al_2O_3	15.06	17.31	17.74	12.89	14.96	14.50	13.26	14.06	15.36	18.22
Fe_2O_3	1.25	2.08	3.54	.89	2.44	4.03	3.19	2.72	3.27	1.07
FeO	1.63	8.13	7.54	1.11	7.03	7.28	9.92	8.34	9.89	5.96
MnO	?	tr	tr	nd	tr	.19	.27	.15	.25	.10
MgO	.05	3.48	3.92	.20	3.86	5.46	7.31	9.72	5.01	tr
CaO	.31	6.77	6.85	.48	6.76	8.46	8.86	11.47	9.47	1.51
Na_2O	6.02	4.14	4.25	3.71	4.95	3.11	2.49	1.89	5.15	4.19
K_2O	5.48	2.87	2.79	5.50	1.64	2.28	3.32	1.43	.19	5.59
H_2O+	.23	.56	.55	.15	.55	3.08	1.35	2.74	3.29	.85
H_2O-	.11	none	none	.08	.09	.36				
P_2O_5	tr	.10	.27	nd	.76	.93	none	none	none	none
S	nd	nd	nd	nd	.05	.18	none	none	none	none
CO_2	none	none	nd	nd	none	3.76	5.20	1.62	2.47	4.75
ZrO_2	.01	nd	nd	nd	.02	nd	none	none	none	none
Totals	99.95	99.14	100.55	100.71	100.16	100.60	100.75	99.26	100.44	100.49

1. Paisanite—Horne Farm Quarry, Red Hill (32, p. 441).
2. Lamprophyre—Black Cascade, Tripyramid Mountain (33, p. 424).
3. Lamprophyre—Norway Rapids, Tripyramid Mountain (33, p. 424).
4. Aplite—southwest slope of Mt. Belknap (31, p. 440).
5. Spessartite—Belknap Mountains (31, p. 455).
6. Camptonite—summit of Mt. Gunstock, Belknap Mountains (31, p. 495).
7. Diabase—Campton Falls, New Hampshire (20, p. 156).
8. Olivine diabase—Campton Falls, New Hampshire (20, p. 150).
9. Diortite—Campton Falls, New Hampshire (20, p. 156).
10. Syenite—Campton Falls, New Hampshire (20, p. 156).

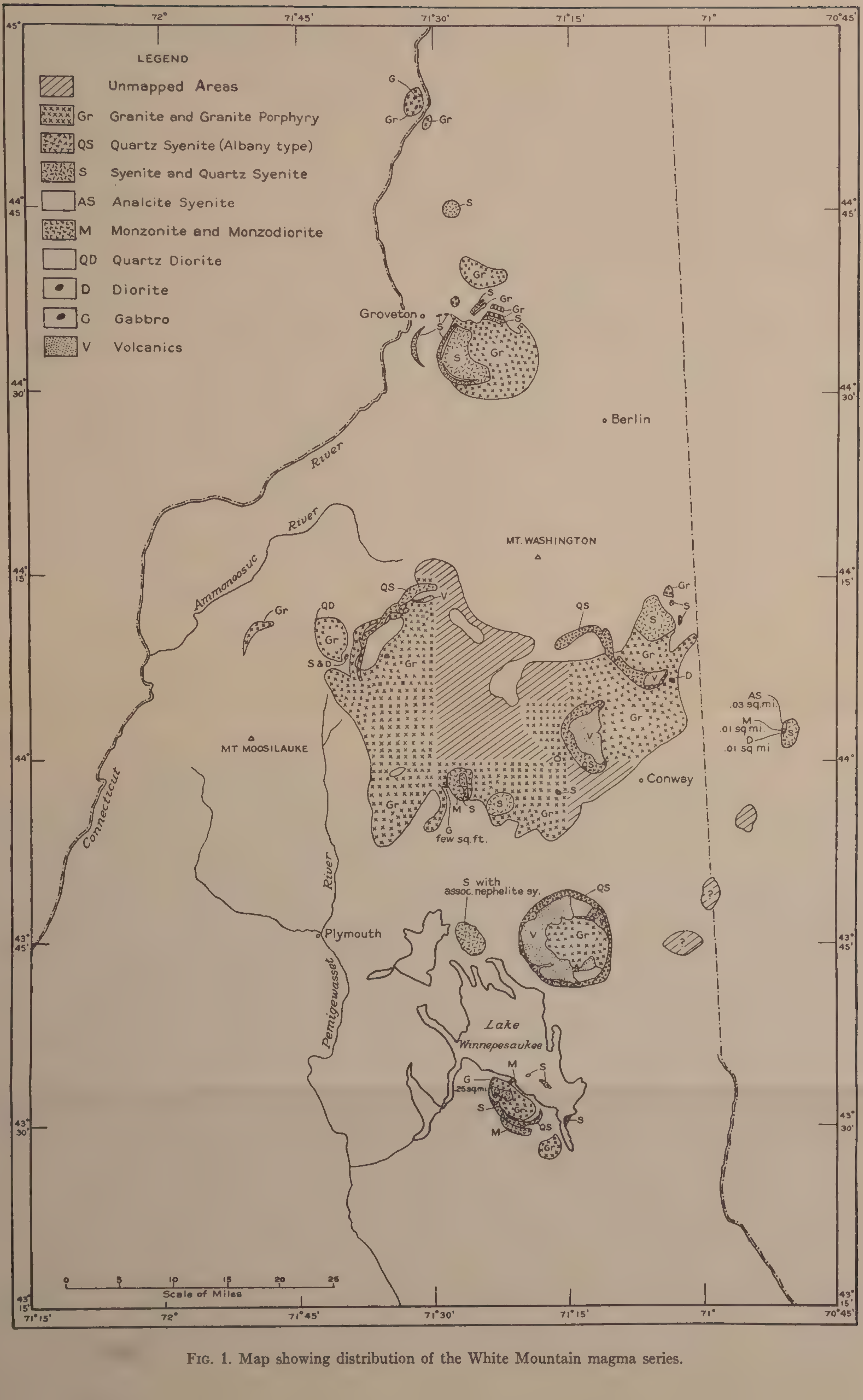

Fig. 1. Map showing distribution of the White Mountain magma series.

Due to the magnitude of the task, the writers have deemed it advisable to confine their studies to the plutonic phases of the White Mountain magma series, and have been forced to neglect the extrusive and dike rocks. A complete theory, however, must ultimately consider these too.

AREAL EXTENT OF PLUTONIC PHASES. The writers have calculated the number of square miles of area underlain by each of the rock types. They have also determined the percentage of each type with respect to the magma series as a whole. The results are shown in Table 4. The figures are given to several decimals in order to represent the rarer types. For the more common types the decimals have no significance. It should be clearly understood that these figures are based only upon those areas studied in recent years, and do not include areas such as the Crawford Notch and Plymouth quadrangles for which sufficient data are not available.

TABLE 4

TABLE SHOWING AREAL EXTENT OF PLUTONIC ROCK TYPES AND PERCENTAGE OF EACH COMPARED TO TOTAL MAGMA SERIES

NAME	SQUARE MILES	PER CENT OF MAGMA SERIES
Granite	315.50	68.9000
Granite porphyry	43.30	9.4300
Quartz syenite (Albany type)	39.90	8.7100
Quartz syenite	7.50	1.5400
Syenite	43.10	9.4100
Analcite syenite	0.03	0.0066
Nephelite syenite	?	?
Monzonite	2.60	0.5700
Monzodiorite	4.00	0.8700
Quartz diorite	1.50	0.3300
Diorite	0.25	0.0546
Norite	?	?
Gabbro	0.10	0.0218
Total	457.78	

The relative proportions of the various rock types as they are seen today in the White Mountain region may not necessarily represent the proportions of those types as magmas. They are rather a function of specific gravities. Granite, being the lightest of the magmas in the region has a greater tendency to rise, and thus, at the present level, is more abundant than any of the other types, whereas gabbro forms only a very minor proportion of those observed at the surface.

Age Relations. The most important data furnished by field relations as to the evolution of the magma series pertains to the relative ages of the different rock types. Although the data from any one area are by no means complete, the facts collected from the whole region indicate that there is a definite succession of rocks beginning with the volcanics.

There is ample evidence that the so-called Moat volcanics are older than most of the plutonic rocks of the White Mountain magma series. In the North Conway quadrangle, all the plutonic phases of the series present, except the diorite, cut the volcanics. In the Ossipee Mountains, the Albany quartz syenite cuts the volcanics and, furthermore, contains inclusions of the latter. On Pleasant Mountain, the volcanics are definitely older than the augite syenites and syenites. Thus, the Moat volcanics are clearly older than the syenites and more siliceous rocks, but, unfortunately, there is no direct evidence as to their age relative to the gabbro, diorite, and monzonite. However, fragments of the plutonics have never been found in the Moat volcanics.

It is certain that the gabbro and diorite of the series are older than the biotite granite since they are cut by the latter in the Belknap Mountains. In the Belknap Mountains, also, some of the diorite occurs as inclusions in the monzodiorite. There are no data on the age of either the norite or quartz diorite. At Pleasant Mountain, the analcite syenite cuts the monzonite and is, in turn, cut by the syenite. The relative age of the nephelite syenite at Red Hill is not known, but until evidence to the contrary is found, it seems probable that it has the same relative age as the analcite syenite of Pleasant Mountain. For the most part, the quartz syenite is younger than the syenite. The Albany quartz syenite is probably essentially contemporaneous with the other quartz syenite. In the North Conway and Percy quadrangles, the latter is found locally grading into the hastingsite granite. In the Percy quadrangle, the hastingsite granite, in turn, grades into the riebeckite granite. Evidence from the Franconia region shows that the granite porphyry is older than the quartz syenite (Albany type) since it is intruded by the latter. In all areas where the Conway biotite granite occurs it is definitely the youngest plutonic present since it cuts most of the other plutonic phases. In most areas, the dikes are younger than the biotite granite, but at Pleasant Mountain, some are older than the diorite.

In summary, the rocks of the White Mountain magma series may be listed chronologically (oldest at bottom) as shown in Table 5. The relative ages of those types shown in brackets are not well known.

TABLE 5

ROCKS OF THE WHITE MOUNTAIN MAGMA SERIES LISTED According to Age (Oldest at Bottom)

Vent agglomerate of the Belknaps	↑ Dikes ↓
Biotite granite	
Riebeckite granite	
Hastingsite granite	
Quartz syenite (Albany type)	
Granite porphyry	
Quartz syenite	
Syenite	
[Nephelite syenite and analcite syenite]	
Monzonite	
Monzodiorite	
[Quartz diorite]	
Diorite	
[Norite]	
Gabbro	
Volcanics—definitely older than syenite and younger rocks. Age relative to analcite syenite and older rocks unknown.	

Inspection of this table shows features which are characteristic of many comagmatic regions. As evolution proceeds, there is a gradual decrease in the percentage of ferromagnesian minerals and anorthite, and a corresponding increase in the alkali feldspars, and, in the final stages, quartz. Chemically this means a decrease in iron, magnesium, and lime and an increase in soda, potash and silica.

LOCUS OF ORIGIN OF ROCK TYPES. It is clear to those who are most familiar with the White Mountain magma series that the different rock types did not originate at the levels where we now see them. They formed at some depth below the present surface of the earth and were then injected into higher levels. Little differentiation took place in the bodies now exposed to view. The evidence for this is that the contacts between different members of the White Mountain magma series are relatively sharp—in many instances they show a knife-edge sharpness. It is true that in some localities gradational contacts exist, but these are usually confined to zones a few feet wide and are insignificant when compared to the size of the rock-bodies as a whole.

Mechanics of Intrusion. It is not the purpose of this paper to discuss the mechanics of intrusion of the White Mountain magma series, but a brief statement is desirable. Evidence from the Ossipee Mountains, North Conway quadrangle, Percy quadrangle, Belknap Mountains, Franconia quadrangle, and Tripyramid Mountain shows that the plutonic rocks of the series occur as stocks and irregular ring-dikes, and that cauldron subsidence has been the dominant mechanism of intrusion.

Minerals

Introductory Statement. Practically all discussions of magmatic differentiation are concerned merely with rock types. The writers are convinced, however, that a far more fundamental study is essential, and that the evolution of the individual minerals must be thoroughly investigated. In this belief, an attempt has been made to determine by chemical and optical methods the composi-

Table 6

Minerals of the White Mountain Magma Series

Olivine Group
  Olivine (hyalosiderite)
  Fayalite

Pyroxene Group
  Diopside-hedenbergite series
  Aegirine series
  Augite
  Enstatite-hypersthene series

Amphibole Group
  Hornblende
  Hastingsite
  Riebeckite

Biotite Group

Plagioclase Group
  Albite
  Oligoclase
  Andesine
  Labradorite

Orthoclase

Anorthoclase

Microperthite

Quartz

Feldspathoids
  Analcite
  Cancrinite
  Nephelite
  Sodalite

Accessories

Allanite
Apatite
Astrophyllite
Fluorite
Ilmenite

Magnetite
Pyrite
Titanite
Woehlerite
Zircon

tion of the essential minerals in all the plutonic phases of the White Mountain magma series. Obviously, to do this by chemical means entirely would be very expensive and laborious. Consequently, certain key minerals have been chosen for chemical analysis and their optical properties determined. From these data, supplemented by information contained in the textbooks of optical mineralogy, it has been possible to determine the chemical composition of most of the minerals in the White Mountain magma series.

A list of the minerals of this magma series is shown in Table 6. The essential minerals are the feldspars, olivines, pyroxenes, amphiboles, biotites, and quartz. Quartz first becomes important in the quartz syenites and granites, although it first appears in the quartz diorite, which is of very limited extent.

FELDSPARS. The usual relations were found in the feldspars—calcic and intermediate plagioclases in the gabbros, diorites, and monzonites; alkali feldspars (albite-oligoclase, orthoclase, anorthoclase, and microperthite) in the monzonites, syenites, and granites.

BIOTITE. Three new chemical analyses have been made of biotites from the White Mountain magma series. One of these is from the gabbro of Tripyramid Mountain, a second is from the monzodiorite of the Belknap Mountains, and a third from the Conway granite of the Percy quadrangle. The chemical compositions and optical data are given in Tables 7 and 8.

It will be observed that in passing from the gabbro to the granite, there is a systematic decrease in silica, titania, alumina, and magnesia, and a systematic increase in ferric iron, ferrous iron, manganese, and lime. The potash and minor oxides are not so regular in their variation. The most striking change is the increase in the iron-magnesia ratio. The available data suggest a continuous reaction series with no sharp discontinuity.

OLIVINE. The olivine (hyalosiderite) in the gabbro of Tripyramid Mountain has been isolated and analyzed. The results are given in Table 7 and the optical properties in Table 8. It is about 40% fayalite and 60% forsterite. Unfortunately, the fayalite from the more siliceous rocks could not be separated for analysis. Optical data had to be employed to determine the chemical composition, and typical data on fayalite from a syenite are given in Table 8. They indicate fayalite, with 10% forsterite and 90% fayalite. As in the biotites, there is a great increase in iron relative to magnesia in going from the basic end of the series to the siliceous. Olivine

Table 7

Chemical Composition of the Minerals of the White Mountain Magma Series

	1	2	3	4	5	6	7	8	9
SiO_2	37.74	35.88	33.48	47.58	46.56	37.40	46.98	34.96	none
TiO_2	5.22	4.17	2.94	.37	1.83	3.20	1.49	none	48.90
Al_2O_3	16.31	14.96	13.64	1.16	2.48	12.34	1.29	none	none
Fe_2O_3	none	2.33	8.00	2.60	6.24	4.16	11.93	none	9.80
FeO	15.52	20.88	23.54	24.21	27.27	25.84	23.38	36.77	38.97
MnO	.06	.18	1.02	.59	1.08	1.24	.24	.52	.36
MgO	14.23	10.04	4.97	3.34	1.35	2.20	.13	27.04	2.03
CaO	.04	.12	.56	18.80	6.15	9.72	1.91	none	nd
Na_2O	.44	.36	.53	.47	4.17	1.80	8.90	nd	nd
K_2O	8.88	9.20	7.80	.21	1.37	1.36	2.74	nd	nd
H_2O+	1.17	.80	2.63	.34	1.27	tr	1.10	nd	nd
H_2O-					nd	.60	none	—	—
F	.45	1.58	.95		—	—	—	—	—
	100.06	100.50	100.06						
Less O for F	.19	.66	.40						
Total	99.87	99.84	99.66	99.67	99.77	99.86	100.09	100.58	100.06

1. Biotite from gabbro (7052)*, Black Cascade, Tripyramid Mountain.
2. Biotite from monzodiorite (609), one-third mile northwest of Ames station, Belknap Mountains.
3. Biotite from granite (19287), granite quarry one mile south of Beech Hill, Percy quadrangle.
4. Hedenbergite from syenite (19258), east slope of knoll south of Burnside Brook at elevation 2160 feet, Percy quadrangle.
5. Hornblende from syenite (19247), in Moore Brook at elevation 2000 feet, Percy quadrangle.
6. Hastingsite from quartz syenite (18299), Jackson Falls, Jackson, North Conway quadrangle (3, p. 110).
7. Riebeckite from granite (19274), ¼ mile N.E. of small swamp on Mill Mt.. Percy quadrangle.
8. Hyalosiderite from gabbro (7052), Black Cascade, Tripyramid Mountain.
9. Ilmenite from gabbro (7052), Black Cascade, Tripyramid Mountain.

* Numbers in parentheses refer to Harvard University rock collections. F. A. Gonyer, analyst of all except specimen 6.

(hyalosiderite) occurs in the gabbro, fayalite in the syenites and granites. Members of the olivine series have not been observed in the diorites or monzonites. There is, apparently, a definite stage corresponding to the intermediate types, in which members of the olivine series could not exist in equilibrium.

Pyroxenes. The pyroxenes of the White Mountain magma series belong to four groups: (1) enstatite-hypersthene, (2) aege-

TABLE 8

OPTICS OF MINERALS OF THE WHITE MOUNTAIN MAGMA SERIES

		1	2	3	4	5	6	7	8	10	11	12	13	14
INDICES	α	1.596	1.599	1.606	1.730	1.688	1.698	1.691	1.721	1.690	1.691	1.687	1.670	1.812
	β	1.656	1.665	1.671	1.736	1.699	1.719	1.694	1.750	1.695	1.698	1.697	—	1.849
	γ	1.656	1.665	1.672	1.755	1.704	1.722	1.699	1.765	1.716	1.718	1.703	1.689	1.860
SIGN		−	−	−	+	−	−	+	−	+	+	−	−	−
OPTIC ANGLE		5°	small	small	60°	35°	47° ± 3°	large	85° ± 2°	60° ± 3°	60°	70°	medium	48°
DISPERSION		$r<v$ weak	$r<v$ —	$r<v$ weak	$r>v$ med.	$r>v$ strong	med. strong	$r>v$ strong	$r>v$ weak	weak	$r>v$ weak	$r<v$ weak	$r>v$ med.	$r>v$ —
ORIENTATION		$X\wedge c=$ 4°	$X\wedge c=$ 3°	$X\wedge c=$ 3°	$Y=b$ $Z\wedge c=$ 45°	$Y=b$ $Z\wedge c=$ 25°	$Y=b$ $Z\wedge c=$ 20°	$Z=b$? $X\wedge c=$ 3°–5°	?	$Y=b$ $Z\wedge c=$ 40°	$Y=b$ $Z\wedge c=$ 43°	$Z=c$	$Y=b$ $Z\wedge c=$ 17°	?
PLEOCHROIM		$Z=Y>X$	$Z=Y>X$	$Z=Y>X$	$Z>Y=Y$	$Z>Y>X$	$Y>Z>X$	$X>Z>Y$				$X=Y=Z$	$Y>Z>X$	

1–8 refer to analyzed specimens—same numbers as in Table 7.
10. Diopside from gabbro (7052), Black Cascade, Tripyramid Mountain.
11. Diopside from syenite porphyry (19665), north peak of Cape Horn, west of Percy quadrangle.
12. Hypersthene from norite (7048), Black Cascade, Tripyramid Mountain.
13. Hornblende from diorite, one mile east of Mt. Pequawket (3, p. 103).
14. Fayalite from syenite (19246), ridge north of Cummings Brook, elevation 1710 feet, Percy quadrangle.

rine, (3) augite, and (4) diopside-hedenbergite. Hypersthene is relatively rare, being found only in the norite of Tripyramid Mountain. Aegerite is also rare, having been observed in a riebeckite granite on Bartlett Haystack in the Crawford Notch quadrangle. Available data indicate that most of the so-called augite in the White Mountain magma series probably belongs to the diopside-hedenbergite series. The problem thus resolves itself into a study of the diopside-hedenbergite series. One new analysis was made for the present paper, the pyroxene from syenite in the Percy quadrangle, which was found to be hedenbergite. This analysis is given in Table 7, the optical properties in Table 8. It is 90% hedenbergite, 10% diopside.

Attempts to obtain clean material for an analysis of the pyroxene of the gabbro from Tripyramid Mountain were unsuccessful. The optics were obtained, however, and are shown in Table 8. Winchell's curve (41, p. 184) indicates that it is diopside-hedenbergite with 68% diopside, 32% hedenbergite.

Optical data were also obtained on pyroxenes from the norite from Tripyramid Mountain, with the results shown in Table 8. According to Winchell's curve (41, p. 177), they indicate a hypersthene with about 24% $FeSiO_3$ and 76% $MgSiO_3$.

In a syenite porphyry from the Cape Horn ring-dike of the Percy quadrangle two pyroxenes were observed. One is very rare and occurs as phenocrysts, the other is in the groundmass. The optical properties of the pyroxene occurring as phenocrysts are given in Table 8. It is very similar to the pyroxene from the Tripyramid gabbro. The groundmass pyroxene, however, is a hedenbergite.

The above facts indicate that the pyroxenes of the White Mountain magma series belong largely to the diopside-hedenbergite series, and that in the gabbro the pyroxene is about 68% diopside, 32% hedenbergite; in the syenite (except for the rare phenocrysts) and granite the pyroxene is about 10% diopside, 90% hedenbergite. There is thus a great increase in iron relative to magnesia in going from the basic to the siliceous end of the series. Since, however, pyroxenes intermediate in composition between those of the gabbro (68% diopside) and the syenite (10% diopside) have not been observed, and since both occur in a syenite porphyry, the former as phenocrysts, the latter as the groundmass, we are led to believe that a discontinuity in the series may exist.

Amphiboles. Three analyses of amphiboles from the White

Mountain magma series are available, two of which are new. One is a soda hornblende from a syenite in the Percy quadrangle and the second is a riebeckite from a riebeckite granite in the same area. A third analysis is of a hastingsite from the North Conway quadrangle. It will be observed that all three are very rich in iron relative to magnesia. Unfortunately, amphiboles in the more basic rocks could not be successfully separated for chemical analysis. Billings (4, p. 293) has shown, however, from a study of the whole New England-Quebec alkaline province that the amphiboles in the basic rocks have a much lower iron-magnesia ratio than those from the siliceous rocks.

The following facts may be noted: (1) Riebeckite is confined to the granites. (2) Hastingsite is confined to the syenites, quartz syenites, and granites. (3) The range of the sodic hornblende is unknown. Riebeckite is younger than hastingsite, for in some specimens the former has been observed as a shell about the latter.

ILMENITE. The opaque mineral ilmenite from the gabbro from Tripyramid Mountain was studied in polished section by the writers, and was found to be a homogeneous ilmenite. This mineral was also separated by the writers and analyzed by F. A. Gonyer; the analysis is given in Table 7.

QUARTZ. Consideration of a number of important facts in regard to the occurrence of quartz may be helpful in explaining later the means whereby it has originated.

In the first place, silica-deficient femags are found mainly in the siliceous rocks. Hastingsite and biotite—both minerals low in silica—are the principal dark minerals of the granites, the rocks in which quartz is most abundant. Such an association strongly suggests that the origin of quartz is in some way related to the crystallization of the silica-poor femags.

Secondly, with the exception of a small body of quartz diorite in the Franconia region, quartz is not present in the White Mountain magma series in any quantity until the quartz syenite stage. It is of the greatest importance to remember that it is also in the syenite stage that hastingsite and fayalite first appear, and pyroxene becomes unimportant.

In the third place, the rocks of the so-called New Hampshire magma series which occur in the same general area as the White Mountain magma series, but are somewhat older, represent a case in point. In these rocks, which include quartz diorite, granodiorite, quartz monzonite, and granite, biotite is the only ferromagnesian mineral present in any amount, and it occurs in all types. In contrast to the White Mountain magma series, quartz appears very early in these rocks. In other words, the appearance of biotite is accompanied by the simultaneous appearance of quartz. This fact alone is strong evidence that quartz is, in part, the result of the crystallization of biotite, a silica-poor femag.

Work by F. S. Miller (27) on the basic rocks of the San Luis Rey quadrangle, California, shows a very similar relation between biotite and quartz. Biotite, which appears in these rocks when the anorthite content of the plagioclase reaches about 56%, is closely accompanied by the appearance of quartz. Apparently, the two are closely related in origin. Miller has further found that many of the gabbroid rocks contain nodular masses composed of pyroxene and calcic plagioclase. These basic nodules grade out into a zone composed of plagioclase, pyroxene, biotite, and quartz. Farther from the center of the nodules the pyroxene has changed to hornblende, and quartz and biotite have become more abundant. The quartz and biotite appear together and increase in amount proportionally.

PART II. THEORY

Theories of Origin of Rock Types

Introductory Statement. Many theories have been developed to explain the great diversity of igneous rocks, particularly in such a consanguineous group as the White Mountain magma series. Some theories are based primarily on differentiation—that is, a primary magma of uniform composition is supposed to break up into subsidary fractions of varying composition. Other theories involve the mixing of two different magmas, or the assimilation of solid rock by magma. Still other theories are based on the melting up of rock in place, either in whole or in part, the latter being known as selective fusion.

Theories of Differentiation. In recent years, a number of theories of differentiation have been presented by petrologists. These include principally liquid immiscibility, gaseous transfer, and fractional crystallization. These theories have been summarized by Daly in his "Igneous Rocks and the Depths of the Earth" (12, pp. 319–332).

According to the theory of liquid immiscibility, differentiation takes place in the magmatic state by the separation of liquid phases of different compositions. The crystallization of these phases gives rise to different rock types. Bowen (7, pp. 7–19) and Grieg (18) have shown, however, that the evidence is decidedly against limited miscibility in natural magmas. Accordingly, we can dismiss this method of differentiation without further comment.

Fenner (14, p. 743) is one of the chief advocates of gaseous transfer. He considers that the gases responsible for differentiation form a separate bubble phase and rise from lower to higher levels in the magma, making selective transfer of materials from lower to higher levels. Bowen (7, pp. 7–19) and others, although realizing that gases may play an important role during the cooling of a magma, believe it very unlikely that notable differentiation of the molten material would accompany this action. The present writers are of the opinion that this process has certainly not been operative to any great extent in the formation of the White Mountain magma series.

Fractional crystallization is the theory of differentiation most widely accepted at present. According to this theory, different rock types are formed by the early crystallization of minerals which are richer in lime, iron, and magnesia than the magma from which they separate. If these minerals are isolated from the magma by gravitative settling or by the squeezing out of the residual magma itself, different rock types are produced. For a more detailed discussion of this theory, the reader is referred to Bowen's "Evolution of the Igneous Rocks" (7).

THEORIES OF ASSIMILATION AND PURE-MELTING. Daly (12, p. 287) has strongly emphasized the importance of both assimilation and pure-melting in the formation of igneous rocks. He defines magmatic assimilation as "the mutual solution of magma with solid rock, with other magma, or with foreign gas, so that a new magma with at least some approach to chemical homogeneity results." In other words, the assimilation of granitic material by gabbroic magma would produce a magma of some intermediate composition. Since differentiation of the syntectic magma accompanies and follows assimilation, the resulting rocks are not the readily identifiable products of addition. Magmatic assimilation may be either high-level or abyssal (intracrustal or in the substratum).

By pure melting the writers mean melting up of older rocks without contamination by magmas, solutions or gases. It may be complete or partial and in the latter case may be called selective fusion. The last minerals to crystallize in the original formation of rocks (quartz and feldspars) would, in general, be the first to go into mutual solution when blocks submerged in a magma reach a level where sufficiently high temperatures are available. The liquid thus formed might either rise as an independent mass because of its low specific gravity or it might become incorporated in the surrounding magma.

THEORIES OF ORIGIN OF ALKALINE ROCKS. A great many theories have been proposed to explain the origin of the alkaline rocks. Among the writers responsible for these are Becke (2), Jensen (24), Evans (13), Goldschmidt (17), Barth (1), Foye (15), Harker (19), Shand (34, 35), Holmes (21, 22), Smyth (36, 37), Gillson (16), Kennedy (25), Daly (11), and Bowen (7). Due to a lack of space none of these will be considered here. For a complete discussion of any of the theories the reader is referred to the above authors.

OUTLINE OF THEORY ACCEPTED. The writers propose to show that none of the processes, outlined above, operating alone is capable of producing the complete White Mountain magma series, but that a combination of fractional crystallization, pure melting, and assimilation is necessary. They will show that, although it is qualitatively possible to produce the White Mountain magma series by fractional crystallization, it is quantitatively impossible.

The writers will first consider the evolution of the minerals of the White Mountain magma series and then the mechanics of differentiation through fractional crystallization. They will then discuss the quantitative difficulties involved in deriving all the rocks by this process alone, and, after a consideration of assimilation and pure-melting, will describe in greater detail the theory accepted.

EVOLUTION OF THE MINERALS OF THE WHITE MOUNTAIN MAGMA SERIES

FELDSPARS. The general variation of feldspar composition is a well-known fact. In the White Mountain magma series, the feldspars follow the general rule, with calcic plagioclase appearing in the gabbro and becoming increasingly richer in alkalies as the rock becomes more siliceous. Alkali feldspars (orthoclase, microperthite, and anorthoclase) first appear in the monzonites, but become abundant only in the syenites and granites. The liquidus-solidus diagram of the plagioclase feldspars is well known, whereby the plagioclase crystallizing from a magma is more calcic than the magma from which it crystallized. The importance of this fact is discussed further on a later page.

BIOTITE, OLIVINE, PYROXENES, AMPHIBOLES. On earlier pages it has been pointed out that the iron-magnesia ratio in the ferromagnesian minerals is much higher in the siliceous rocks of the White Mountain magma series than in the basic. J. H. L. Vogt has made similar observations: "The low-melting components of the ferro-magnesian silicates which are rich in iron and the low-melting albite component of the plagioclase are all enriched in the rocks of the rest-magma direction" (39, p. 123). In an even earlier paper (38, pp. 151–152) he gave reasons for believing that the liquidus-solidus curve of the olivine series is similar to that of the plagioclase series. This deduction has been confirmed by recent experimental work by Bowen and Schairer (8, p. 153).

A diagrammatic curve for olivine, pyroxene, and biotite, similar to the liquidus-solidus curve for plagioclase feldspar is shown in Figure 2. It is intended to show that the magnesia-iron ratio is much higher in the solid phase than in the liquid phase with which it is in equilibrium. If complete reaction occurs, the final solid phase will have the same composition as the original liquid. If, however, reaction is incomplete, the final liquid will have a lower magnesia-iron ratio than the original liquid. Differentiation will proceed, therefore, in the direction of rocks with a low magnesia-iron ratio. The amphiboles will follow the same general rules.

QUARTZ. It has been pointed out that (1) the silica-deficient femags of the White Mountain magma series are found mainly in the most siliceous rocks, (2) quartz does not appear in any quantity in the White Mountain magma series until the quartz syenite stage, (3) in the older New Hampshire magma series, biotite and quartz appear very early in the evolution of the series, and (4) in the San Luis Rey quadrangle of California biotite and quartz appear simultaneously.

These facts indicate that the formation of free silica in the White Mountain magma series is, at least in part, related to the evolution of silica-poor dark minerals. It is, apparently, a process taking place in the late stages of differentiation. The writers believe that in the late stages of the evolution of the White Mountain magma series potential metasilicates, such as members of the diopside-hedenbergite series and common hornblende broke down to give orthosilicates such as fayalite, hastingsite, and biotite, with the release of free silica to form quartz. The alkali feldspars were also involved in this process in certain reactions also with the release of free silica. By further fractional crystallization, a relatively small amount of quartz might be concentrated to form granites.

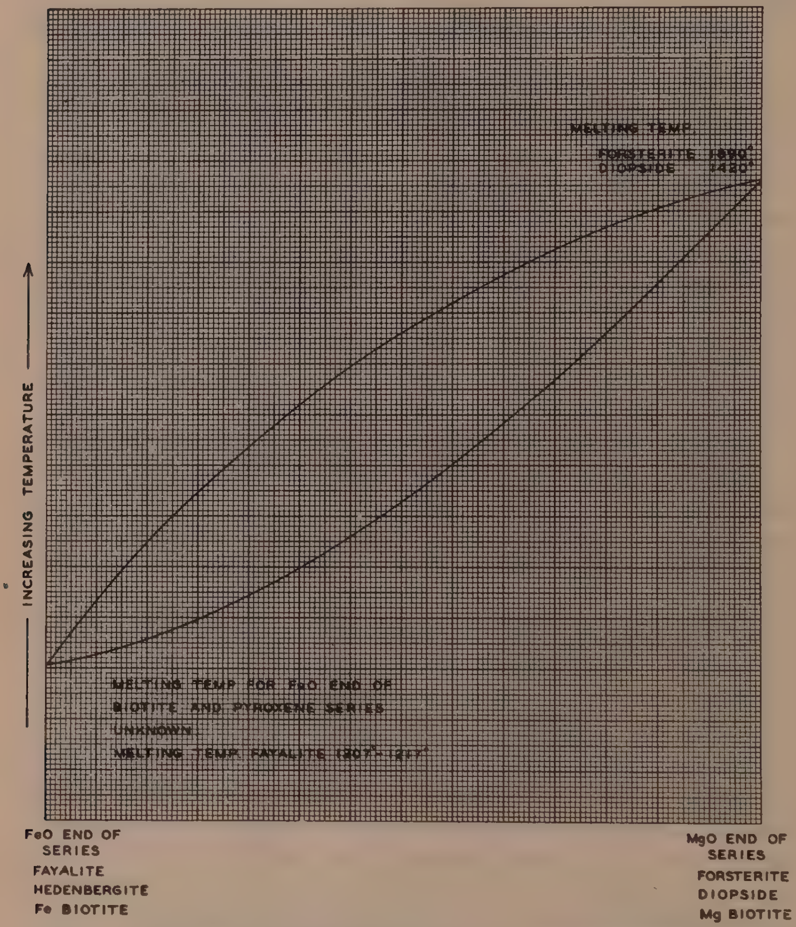

FIG. 2. Diagrammatic liquidus-solidus cure for forsterite-fayalite, diopside-heden-bergite, and biotite series. Modified after Vogt. Since this figure was prepared Bowen and Schairer have presented a similar diagram (8).

THEORETICAL EVOLUTION OF THE WHITE MOUNTAIN MAGMA SERIES BY FRACTIONAL CRYSTALLIZATION

PROCESS. Let us summarize, in the light of the above facts, the theoretical evolution, by fractional crystallization, of a gabbroic magma such as that which gave rise to the White Mountain magma series. To begin with, we may assume a great chamber of gabbro, some distance below the surface, which is in the process of cooling. As cooling proceeds, olivine, pyroxene, and calcic plagioclase begin to crystallize first. In this early stage of differentiation it is obvious that the ferromagnesian minerals separate out in far greater proportion than in the later stages, since the amount of dark minerals in each succeeding rock type has become less and less. Whether or not there is opportunity for reaction between the magma and these early-formed crystals is of the greatest importance. Since crystallization, with perfect reaction, of a gabbroic magma would result in the formation of a gabbro, it is evident that in the production of the observed series, reaction has not been complete.

The minerals which crystallize early, having a specific gravity which is generally greater than the liquid, tend to settle into the depths. The residual liquor left behind now has a different composition than at first. Intrusions of the magma into the country rock, which would originally have resulted in gabbro, now produce some such rock as diorite. Further crystallization and settling of minerals causes the magma to become progressively less mafic until it has finally attained the composition of a granite. Intrusion of the magma at appropriate intervals produces the various rock types of the series.

The chemical changes which take place in the magma during the course of differentiation are of fundamental importance. These include: (1) a decrease in the amount of lime and an increase in the amount of alkalies in the magma, (2) the enrichment of the magma in iron relative to magnesia, and (3) the absolute enrichment of the magma in silica, especially in the late stages of differentiation.

The decrease in the amount of lime is due, as we have seen, to the early separation of calcic plagioclase and pyroxene. Calcic plagioclase and sodic plagioclase form a continuous reaction series and the early crystallization of the former causes the magma to become enriched in the latter. The amount of potash is also increased in the magma as differentiation proceeds. The more calcic plagioclase is found, accordingly, in the less siliceous rocks, whereas the soda and potash feldspars are concentrated in the late differentiates.

Accompanying this process is the steady increase in the amount of iron relative to magnesia from the more mafic rocks to the granites. We have already considered the means by which the change takes place. It is the result of the early separation of minerals of the biotite, olivine, and pyroxene series which are high in magnesia relative to iron (magnesia-rich biotite, hyalosiderite, and diopside). This causes a relative increase in the iron-magnesia ratio of the magma itself. As crystallization proceeds, the minerals formed become relatively poorer in magnesia and relatively richer in iron, until in the late stages (syenites and granites) they are high in iron compared to magnesia (iron-rich biotite, fayalite, and hedenbergite). There is evidence that there is a similar iron-magnesia-ratio change in the hornblende system.

The rather sudden increase in the silica content of a magma by differentiation has already been pointed out. As a rule, quartz first appears in the White Mountain magma series in the syenite stage. It is also in this stage that hedenbergite and silica-deficient hastingsite first appear, and the possible origin of quartz by reactions involving these minerals has been considered. In the granites, quartz is present in great abundance. The fact that it is accompanied by biotite and hastingsite (minerals low in silica) suggests that it is, in part, closely related in origin to these two minerals.

By thus emphasizing the simultaneous appearance of silica-deficient femags with quartz in the later stages of the evolution, the writers do not wish to imply that silica-deficient femags are confined to the siliceous end of the series. Olivine is found in the gabbro, and biotite appears all through the series.

DERIVATION OF ROCK TYPES. It is possible to derive the series from gabbro through monzonite, syenite, and granite by the subtraction of crystals as shown below in Table 9. There are several primary assumptions on which the development of this series is based. In the first place, in order to simplify the method, biotite was omitted all the way through the calculations, largely because it is in general a late mineral to crystallize. Secondly, as shown in the liquidus-solidus diagram for the plagioclases, the feldspar which crystallized in a given magma will be richer in anorthite than the magma. For this reason, a feldspar more calcic than the normal plagioclase of the magma was subtracted in each case. A similar relation holds for the iron-magnesia ratio of the ferromagnesian minerals. This is brought out in the curve shown in Figure 2. Thus, in each case, a ferromagnesian mineral was subtracted which had relatively more magnesia to iron than the normal mineral for the rock type. Otherwise, the minerals subtracted had the compositions of the analyzed minerals of the various rocks, as shown above. Ferric iron has been converted to ferrous iron so that the iron could be handled as a total in the ferrous state. Minor constituents have been omitted from the calculations.

TABLE 9

DERIVATION OF ROCK TYPES FROM A GABBRO MAGMA BY FRACTIONAL CRYSTALLIZATION

(For details see text)

	GABBRO	MONZONITE	SYENITE	GRANITE
SiO_2	48.04%	58.00%	63.60%	71.40%
TiO_2	2.56	1.38	.61	.55
Al_2O_3	20.10	16.10	16.20	14.32
FeO	8.21	6.45	4.05	2.10
MgO	4.68	2.03	.80	.21
CaO	11.52	7.82	3.13	2.10
Na_2O	3.01	4.60	6.04	3.31
K_2O	.79	3.69	5.66	5.78
Total	98.91%	100.07%	100.09%	99.77%

MINERALS SUBTRACTED TO CHANGE:

	GABBRO TO MONZONITE	MONZONITE TO SYENITE	SYENITE TO GRANITE
Orthoclase	— %	— %	20.02%
Albite	17.00	5.24	19.91
Anorthite	36.00	11.95	5.00
Pyroxene	10.00	16.00	—
Olivine	10.00	—	—
Ilmenite	4.50	2.00	—
Hastingsite	—	—	13.00
Total	77.50%	35.19%	57.93%

The development of this series was accomplished by starting with the analyzed gabbro and subtracting minerals present in the gabbro, with the qualifications given above. The resulting rock was a typical monzonite. By repeating the process, a syenite and a granite were derived. All of the calculations were made on the basis of molecular proportions. The following table shows the analyses of the rocks and the minerals subtracted to form the rock next in the series. Under the gabbro, the minerals subtracted to form the monzonite are given; the derived monzonite analysis is shown and below that, the minerals subtracted to form the syenite et cetera.

On the way through this series the diorite and monzodiorite would be developed, and by a similar process the biotite granites would be formed from the hastingsite granite.

The analcite and nephelite syenites are definitely off the main line of descent shown in the above table. Special conditions are necessary to explain their presence. Both of these rocks form small bodies and there is no available field evidence which offers a clue as to their origin. Daly (12, p. 510) has suggested the possibility of the assimilation of lime-bearing rocks in the region, but does not exclude the possibility of the role of gaseous transfer. A third method by which these rocks might be formed, which would be consistent with fractional crystallization, is based upon Bowen's theory of the incongruent melting of orthoclase to form felds- pathoids.

Quantitative Difficulties. An objection to the derivation of the various rock types of the White Mountain magma series by fractional crystallization is based on the belief that tremendous quantities of gabbro would be necessary to produce the syenites and granites, and, thus, there should be large quantities of basic rocks beneath the White Mountain area. According to isostasy, such a region should be a lowland and not a mountainous area. It is possible to compute roughly the necessary quantity of gabbro to produce the known rocks of the White Mountain magma series. This may be done in several ways, one of which is by direct application of the figures in Table 9. There can be little doubt that the plutonic bodies observed at the surface extend down at least a mile, and probably much farther. We may thus readily calculate the volume of the various plutonic bodies in the uppermost mile of the earth's crust, for the areal extent in square miles in that case is equivalent to the volume in cubic miles.

Since the known areal extent of the granite and granite porphyry is 358.8 square miles, there would be 358.8 cubic miles of granite and granite porphyry. Referring to Table 9, if 77.5% of the gabbro is removed, the remaining 22.5% is monzonite; if 35.19% of that is removed, 14.9% of syenite remains; 57.93% of the constituents of the syenite removed leaves 6.3% of granite. Thus, to produce 358.8 cubic miles of granite, 5700 cubic miles of gabbro would be necessary. Similarly, 90.5 cubic miles of syenite and quartz syenite would require 607 cubic miles of gabbro, and 2.6 cubic miles of monzonite would require 11.5 cubic miles of gabbro. Thus, to produce all of the rock types by fractional crystallization of a gabbro, 6318 cubic miles of gabbro would be required. If this gabbro were spread out under the whole area shown in Figure 1—about 9000 square miles—it would have a thickness of 0.7 miles.

These figures, however, give a minimum. They assume an efficiency which undoubtedly does not exist. In the second place, these figures are based on the assumption that the plutonic rocks of the magma series are only one mile in thickness. The differentiates are probably actually more than a mile thick. It is doubtful, nevertheless, if they ever extended very high above their present highest point. Some of the coarse plutonic phases hold up mountains which are only about 1000 feet lower than the highest point in the region (Mount Washington, 6290 feet). Billings (3, p. 128) has shown that the surface on which the volcanic members of the magma series were deposited was at least a little higher than Mount Washington and possibly much higher. Assuming that the ancient surface was a mile or more above Mount Washington, the plutonic rocks could not have extended very far above their present highest position since coarsely crystalline rocks cool at some depth. There is no means, however, of knowing the depth to which the plutonic differentiates extend. It seems logical to assume, however, that these rocks probably extend at least 3 or 4 miles below the present surface. If the mechanics of ring-dike intrusion as outlined by Anderson (10) are correct, the vertical dimension of a ring-dike would be approximately the same as the diameter of the ring itself. In view of this fact, the plutonics of the ring-dikes and associated stocks might extend down at least 8 or 10 miles.

If the above facts are true, a tremendous quantity of parent gabbroic magma would be required. The total area of the map (Figure 1) showing the White Mountain magma series is 9000 square miles. If the magma were confined entirely beneath the area covered by this map, it would extend all the way to the basaltic substratum. It is difficult to understand how so much gabbroic rock could now underlie this part of New England and yet allow the country to stand so high isostatically. Furthermore, there is some question as to whether the relatively thin crust would have been stable over such a large molten mass.

Assimilation and Pure-melting. Consideration of the effects of assimilation in producing rock types involves several factors. The depth at which the process takes place, the character of the material to be assimilated, the chemical composition of the magma, and the temperature of the magma all play important parts in the process. Conditions become more favorable for assimilation with increasing depth, higher initial temperature and lower melting temperature of the assimilated material, and increasing temperature of the magma. Thus, with sufficient depth and temperature, there can be no doubt as to the effectiveness of assimilation. Assimilation alone will not explain the character of the rocks observed in the White Mountain magma series. By the assimilation of siliceous sediments and granites it would be possible to account for a series from gabbro through possibly monzodiorite, but to produce the syenites and granites, it would be necessary to assimilate prohibitive amounts of material. Moreover, mixing an older granite with gabbro could never produce a granite.

Many of the objections to assimilation, such as the heat problem, also apply to pure-melting as the sole means of deriving the White Mountain magma series. Pure-melting may be complete or partial. Complete melting of older rocks can not explain the series. There are no known older rocks in the region with the same composition as the White Mountain magma series. Moreover, in complete melting granite would be generated first, gabbro last and the sequence would be precisely the reverse of that observed. Selective fusion of older rocks as the sole process is also eliminated for the last reason given above.

THEORY OF ROCK EVOLUTION ACCEPTED

From a consideration of all the foregoing facts, it appears that although fractional crystallization alone is qualitatively capable of producing all the rock types of the White Mountain magma series, quantitatively it is not adequate. Too great an amount of the parent magma is required to produce all the siliceous differentiates. It has also been shown that assimilation alone cannot possibly explain the origin of certain of the more siliceous rocks of the series, and that pure-melting as the sole process is open to the same objections as assimilation and to several others. In view of these facts, the writers have concluded that fractional crystallization and assimilation have gone on together with selective fusion, and that each has helped to produce the rock sequence of the magma series.

Qualifications as to the depth at which differentiation by fractional crystallization took place are necessary. According to Stokes' Law, and assuming that the viscosities given by Daly (12, p. 193) for moderate depths in the earth are of the right order of magnitude, the rate of settling of an olivine crystal 0.5 mm. in diameter, at depths of from 30 to 40 miles in the crust, is practically negligible in the time available. Thus, fractional crystallization becomes important only at some distance above the substratum. It is impossible to calculate this distance because there are no available data on viscosities at various depths in the crust.

On the basis of the facts and assumptions discussed above, the evolution of the White Mountain magma series is believed to have resulted from the invasion of the crust by basaltic magma, largely by stoping; melting and assimilation of the stoped blocks; and fractional crystallization of the original magma and the liquids formed by melting and assimilation. The evolution was complex in that these processes were operating essentially simultaneously at different levels in the crust. At the deeper levels, pure-melting and assimilation were important, because there sufficient heat was available for those processes. Higher in the crust, fractional crystallization was going on—at first in the basaltic magma alone, and later in the liquids formed by selective fusion and assimilation, which moved upward continuously as they formed. The gabbros and diorites were probably derived directly from the original basaltic magma, but the other rock types resulted from fractional crystallization of the original magma contaminated by assimilated and melted older rocks. The sequence, however, was definitely controlled by fractional crystallization.

The syntectic magma underwent fractional crystallization and differentiation in the following way. Due to early separation of calcic feldspars and a failure of reaction, the alkali feldspars concentrated in the late differentiates. Similarly, due to the separation of magnesia-rich ferromagnesian minerals, iron increased relative to magnesia in the later differentiates. Quartz had a dual origin. In part it appeared due to the separation of silica-deficient femags. Much of the quartz, however, is merely older quartz which was present in the pre-existing granites and schists, was incorporated in the syntectic magma and then concentrated in the later differentiates.

NATURE OF THE MAGMA CHAMBER

The exact size, shape and location of the chamber or chambers in which differentiation occurred is problematical. One hypothesis pictures a single, large chamber, roughly circular in ground-plan and underlying practically all of central and northern New Hampshire and part of eastern Vermont and western Maine. Locally, however, there were cupolas extending up from the main chamber to within a few miles of the surface. These cupolas, which existed directly beneath the areas now containing rocks of the magma series, were the chief agents localizing the cauldron subsidence and igneous intrusion. An alternative theory is possible. It may be assumed that instead of one large magma chamber at depth with cupolas extending up from it, there was a separate, narrow, cylindrical chamber underlying each local area of intrusion.

FUTURE WORK

The problem of the evolution of the White Mountain magma series is, of course, intimately tied up with similar problems in other areas. Information gathered elsewhere will shed light on our problem in the White Mountains. The work of the Geophysical Laboratory at Washington is also of prime importance, and gives us much of our most significant data. More specifically in the White Mountain district the following additional data should be gathered:

(1) Analyses of more minerals, particularly those ends of the pyroxene, amphibole, and olivine series which are as yet not analyzed. The writers are of the opinion that additional mineral analyses are of much more importance than rock analyses.

(2) Additional field data on the age relations of the plutonic rocks. The chronological position of some of the intrusive rocks is still unknown.

(3) Additional data on the size, shape, and mechanics of intrusion of the rock bodies. Large areas of the White Mountain magma series are exposed in the Crawford Notch, Plymouth, and Mount Washington quadrangles, but they have not been studied since the Hitchcock Survey sixty years ago. The Division of Geological Sciences of Harvard University will probably undertake this study during the next few years.

(4) The importance of deuteric and hydrothermal processes should be considered much more fully.

(5) The genetic relations of the volcanic and dike rocks to the plutonics must be considered.

(6) Seimological and other data may give more information as to the depths to which the granite and syenite masses extend.

Physical data of importance include:

(1) Viscosity of magmas under high pressure, in order to determine the rate of crystal settling under the influence of gravity.

(2) Investigation in the laboratory of the presumed liquidus-solidus relation existing between iron and magnesia in the ferromagnesian minerals as proposed in this paper.

BIBLIOGRAPHY

1. Barth, T. F. W., Die Pegmatitgange der taledonischen Intrusivgesteine im Seiland-Gebiete: *Skrift. Norsk. Videnskaps Akad.*, no. **8**, Oslo, 1927.
2. Becke, F., Die Eruptivgebiete des Bohm. Mittlegebirges und der Amerik. Andes: T.M.P.M., vol. **22**, p. 247, 1903.
3. Billings, M. P., The Petrology of the North Conway Quadrangle in the White Mountains of New Hampshire: *Proc. Am. Acad. Arts Sci.*, vol. **63**, no. 3, pp. 67–137, map, 1928.
4. Billings, M. P., The chemistry, optics and genesis of the hastingsite group of amphiboles: *Am. Mineral.*, vol. **13**, pp. 287–296, 1928.
5. Billings, M. P., Paleozoic Age of the Rocks of Central New Hampshire: *Science*, vol. **79**, pp. 55–56, 1934.
6. Billings, M. P., Geology of the Littleton and Moosilauke Quadrangles, New Hampshire, *in preparation.*
7. Bowen, N. L., The Evolution of the Igneous Rocks, *Princeton*, **1928.**
8. Bowen, N. L., and Schairer, J. F., The System MgO-FeO-SiO_2: *Am. Jour. Sci.*, 5th. Ser., vol. **29**, pp. 151–217, 1935.
9. Chapman, R. W., Geology of the Percy Quadrangle, New Hampshire: *Doctorate thesis*, Harvard University, **1934.**
10. Clough, C. T., Bailey, E. B., Wright, W. B., and Others, Tertiary and Post-Tertiary Geology of Mull: *Mem. Geol. Soc. Scotland*, **1924.**
11. Daly, R. A., Origin of the Alkaline Rocks: *Bull. Geol. Soc. Am.*, vol. **21**, pp. 87–118, 1910.
12. Daly, R. A., Igneous Rocks and the Depths of the Earth. McGraw-Hill Book Co., *New York*, **1933.**
13. Evans, J. W., The Origin of the Alkaline Rocks: *Geol. Mag.*, vol. **57**, p. 559, 1920.
14. Fenner, C. N., The Katmai Magmatic Province: *Jour. Geol.*, vol. **34**, no. 7, pp. 673–772, 1926.
15. Foye, W. G., Nephelite Syenites of Haliburton County, Ontario: *Am. Jour. Sci.*, p. 413, **1915.**
16. Gillson, J. L., On the Origin of Alkaline Rocks: *Jour. Geol.*, vol. **36**, no. 5, pp. 471–474, 1928.
17. Goldschmidt, V. M., Stammentypen der Eruptivgesteine: *Videns. Skrift. I, Mat.-Naturv. Klasse*, no. **10**, pp. 1–11, 1922.

18. Grieg, J. W., Immiscibility in Silicate Melts: *Am. Jour. Sci.*, 5th. ser., vol. **13,** pp. 1–14, 133–154, 1927.
19. Harker, A., The Natural History of Igneous Rocks, *New York*, **1909.**
20. Howes, G. W., On a group of dissimilar eruptive rocks in Campton, New Hampshire: *Am. Jour. Sci.* 3rd. ser. vol. **17,** pp. 147–151, 1879.
21. Holmes, A., The Tertiary Volcanic Rocks of the District of Mozambique: *Quart. Jour. Geol. Soc.*, p. 252, **1916.**
22. Holmes, A., and Harwood, Volcanic Rocks Near Ruwenzori: *Quart. Jour. Geol. Soc., London*, pp. 370–442, **1932.**
23. Jenks, W. F., Petrology of the Alkaline Stock at Pleasant Mountain, Maine, *Am. Jour. Sci.*, vol. **28,** pp. 321–340, 1934.
24. Jensen, H. I., The Distribution, Origin, and Relationships of the Alkaline Rocks: *Proc. Linn. Soc. N. S. Wales*, vol. **33,** pp. 585–586, 1908.
25. Kennedy, W. Q., Trends of Differentiation in Basaltic Magmas: *Am. Jour. Sci.*, vol. **25,** no. 147, pp. 239–256, 1933.
26. Kingsley, L., Cauldron-Subsidence of the Ossipee Mountains: *Am. Jour. Sci.*, 5th. ser., vol. **22,** pp. 139–168, 1931.
27. Miller, F. S., Petrology of the San Marcos Mountain Gabbro, San Luis Rey Quadrangle, California: *Doctorate thesis*, Harvard University, **1934.**
28. Modell, D., The Geology and Petrology of the Belknap Mountains Area, New Hampshire, *Doctorate thesis*, Harvard University, **1933.**
29. Page, A., Geology of the Sandwich Range, New Hampshire, *in preparation.*
30. Perry, J. H., Notes of the Geology of Mt. Kearsarge: *Jour. Geol.*, vol. **11,** pp. 403–412, 1903.
31. Pirsson, L. V., and Washington, H. S., Contributions to the Geology of New Hampshire, I, Geology of the Belknap Mountains: *Am. Jour. Sci.*, 4th. ser., vol. **20,** pp. 344–352, 1905; vol. **22,** pp. 439–457, 493–514, 1906.
32. Pirsson, L. V., and Washington, H. S., Contributions to the Geology of New Hampshire, III; On Red Hill, Moultonboro: *Am. Jour. Sci.*, vol. **23,** pp. 257–276, 433–447, 1907.
33. Pirsson, L. V., and Rice, W. N., Contributions to the Geology of New Hampshire, IV, Geology of Tripyramid Mountain: *Am. Jour. Sci.* 4th. ser., vol. **31,** pp. 269–291, 405–431, 1911.
34. Shand, S. J., The Problem of the Alkaline Rocks: *Proc. Geol. Soc. So. Africa*, pp. 19–32, **1922.**
35. Shand, S. J., Limestone and the Origin of Feldspathoidal Rocks: *Geol. Mag.*, vol. **67,** no. 795, Sept. 1930.
36. Smyth, C. H., Chemical Composition of Alkaline Rocks, and its Significance as to their Origin: *Am. Jour. Sci.*, 4th. ser., vol. **36,** pp. 34–36, 1913.
37. Smyth, C. H., The Origin of Alkaline Rocks: *Am. Phil. Soc. Proc.* vol. **66,** 1927
38. Vogt, J. H. L., Die Silikatschmelzlasungen, I, Über die Mineralbildung in Silikalschmelzlasungen: *Videns. Skrift. I, Math. Naturv. Klasse*, no. 8, 1903.
39. Vogt, J. H. L., The Physical Chemistry of the Magmatic Differentiation of Igneous Rocks: *Videns. Skrift., I. Math. Naturv. Klasse*, no **15,** pp. 123–128, 1924.
40. Williams, C. R., Geology of the Franconia Region, New Hampshire: *Doctorate thesis*, Harvard University, **1934.**
41. Winchell, A. N., Elements of Optical Mineralogy, Pt. II, pp. 424, John Wiley and Sons, *New York*, **1927.**

NOTES AND NEWS

SPECTROGRAPHIC ANALYSIS OF TOURMALINES WITH CORRELATION OF COLOR AND COMPOSITION

T. W. Warner, Jr., *Pomona College, Claremont, California.*

Previous work on the subject of tourmaline analysis in an endeavor to associate chemical composition with color has been reported by Wild,[1] Riggs,[2] Bastin,[3] and discussed by Doelter.[4] A number of non-spectrographic chemical analyses are tabulated by Doelter[4] and Dana.[5] In an article by Holden,[6] the color of rubellite is attributed to a manganese content of $0 \cdot X$-2% Mn_2O_3.

The spectrographic examinations were made by means of a large Gaertner quartz spectrograph,[7] using a slit width of 0.035 mm. W. and W. panchromatic plates were used to photograph the visible spectra and Eastman D. C. ortho plates for the ultra-violet. By this means the spectral range was covered from 7000 Å to 2400 Å. A 100 volt direct current arc which drew 18 amp. on a closed circuit was used to excite the spectra. Acheson purified graphite electrodes, 3/8″ in diameter, were used.

The samples of tourmaline were very carefully chosen from flawless material, the color ranging from very dark green to red. In some cases where flawless material was unobtainable in the rough crystals, cut stones were used. In so far as was possible careful attention was given to avoid using zoned crystals. In the case of bi-colored samples, however, it was found that in every case the material was zoned to some slight extent along the *c*-axis. In these cases the sample was selected from the core of the crystal avoiding contamination as much as possible.

Each sample was prepared by the following procedure: First, the crystal was inspected for general suitability, such as clarity,

---

[1] Wild, *Centr. Mineral. Geol.*, Abt. A, **1931**, pp. 327–33.

[2] Riggs, The Analysis and Composition of Tourmaline; *Am. Jour. Sci.*, (3) vol. **35**, pp. 35–51, 1888.

[3] Bastin, Geology of the pegmatites and associated rocks of Maine: *U. S. Geol. Survey*, Bull. **445**, 1911.

[4] Doelter, *Handb. Mineralchemie*, **11**, 2, pp. 749–788.

[5] Dana, *System of Mineralogy*, 6th Ed., p. 642.

[6] Holden, *Am. Mineral.*, vol. **9**, pp. 101–8, 1924.

[7] Spectrographic examinations were made in one of the Pomona College Laboratories using apparatus and technique customarily employed by Dr. Theodore Kenard.

TABLE 1

Spec. No.	1	2	3	4	5	6	7	8	9	10	11	12	13	14	15
ELEMENTS															
Li	Vs	Vs	S	S	S	Vs	Vs	Vs	Vs						
Na	Vs	Vs	Vs	Vs	Vs	Vs	Vs	Vs	Vs						
Mg	tr	tr	tr	tr	tr	tr	tr	tr	tr	tr	tr	S	tr	tr	tr
Ca	trtr	trtr	trtr	trtr	trtr	trtr	trtr	trtr	trtr						
Al	M	M	M	M	M	M	M	M	M	M	M	M	M	M	M
B	M	M	M	M	M	M	M	M	M	M	M	S	M	M	M
Cu	tr	Vs	tr	—	—	trtr	trtr	trtr—	trtr	tr	tr	Vs	trtr+	trtr	tr
Fe	trtr—	M	trtr—	S	S	S	—	tr—	Vs	M	S+	S—	Vs	trtr	tr
Ga	tr	trtr	tr	tr	tr	trtr	tr	trtr	tr	tr	tr	tr	tr	tr	tr
Mn	tr	Vs+	Vs—	Vs	S	Vs	tr++	Vs	Vs	tr	Vs—	tr	Vs	S	Vs
Pb	tr	tr	—	tr	trtr	—	Vs	tr	tr	tr	tr—	Vs—	tr	Vs—	tr
Si	M+	M+	M+	M+	M+	M+	M+	M+	M+	M+	M+	M+	M+	M+	M+
Sn	Vs	trtr	—	trtr	tr	tr	S	tr	tr	trtr	tr	trtr	tr	trtr	trtr
Ti	trtr	trtr	—	—	—	trtr	trtr	tr	tr	tr	tr	tr	trtr	—	—
V	trtr— —	trtr— —	trtr— —	trtr— —	trtr— —	trtr— —	trtr— —	trtr— —	trtr— —	trtr— —	trtr— —	trtr— —	trtr— —	trtr— —	trtr— —
Be	—	—	—	—	—	S	—	—	—	—	—	—	—	—	—
Locality	S.D.	Brazil	S.D.	S.D.	S.D.	S.D.	S.D.	S.D.	S.D.	S.D.	S.D.	S.D.	S.D.	S.D.	S.D.

KEY TO CHART SYMBOLS: trtr—very minute trace tr—trace Vs—very small S—Small M—Medium S.D.—San Diego

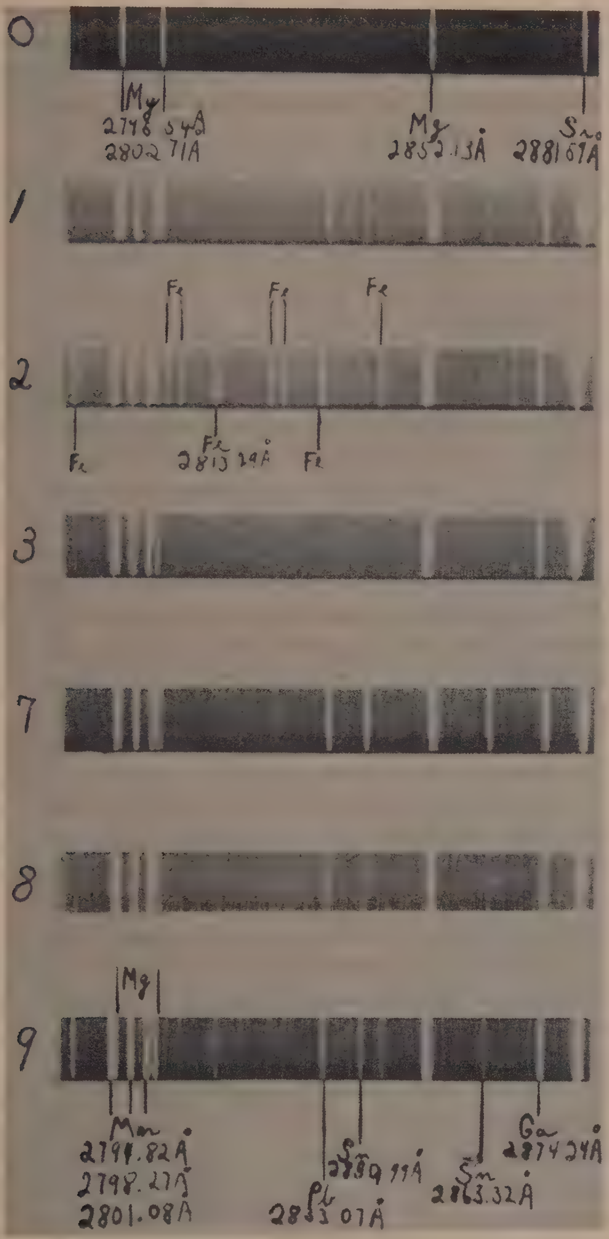
0
Mg
2778 54Å
2802 71Å
Mg
2852.13Å
Sn
2881 67Å
1
Fe
Fe
Fe
2
Fe
Fe
2813 29Å
Fe
3
7
8
Mg
9
Mn
2794.82Å
2798.27Å
2801.08Å
Pb
2833 07Å
Sn
2839 99Å
Sn
2863.32Å
Ga
2874 24Å

FIG. 1

zoning, and surface deposit. It was then crushed by wrapping carefully in paper and striking it with a hammer. This precaution was a vital necessity to avoid any iron contamination which might in any way develop. The pieces thus obtained were selected individually using a 10 power binocular microscope. The particles were handled by tweezers which had been dipped in "air-plane dope," the substance which was found to be the safest in avoiding contamination. The selected particles were then ground in a thoroughly cleaned new agate mortar. Paraffin shields were made which fitted snugly to the sides of the mortar, preventing the material from being scattered or contaminated. The crushing process was continued until the tourmaline was reduced to a coarse powder. The powder thus obtained was again examined under the microscope and any suspicious particles were removed. The sample was then carefully measured and loaded on the electrode by means of a paper chute, the electrode having been previously hollowed at the tip so as to collect the material and prevent dispersion on arcing.

In photographing the visible spectra, an exposure of 30 seconds was given. A 40 second exposure was used in the ultra-violet. Three consecutive exposures were made of each sample in each case. Before volatilizing any sample, the spectrum of the electrodes was taken so as to avoid any confusion in the interpretation of the plates. Fifteen samples were studied and fifty-two elements were tested for. A large piece of the original crystal, or in the case of the cut stones an exact duplicate of the specimen used, was retained for color comparison. The plates thus obtained were interpreted by means of dilution standards.[8] Traces as slight as .0005% were noted.

The object of this investigation was to discover, if possible, what elements were responsible for the various colors in tourmaline. (See table 1.) Figure 1 shows an enlargement of the spectra, 0 being the blank arc while Nos. 1, 2, 3, 7, 8, and 9 correspond to the respective samples.

One fact definitely established is that the iron content varies directly and proportionately with the depth of color in the greens, and inversely in the pinks and reds, being totally absent, or, if present, only in extremely minute traces in the reds. The darker greens had the most iron, the content becoming less in the lighter shades, but never becoming as slight as the content of even the lightest pink.

---

[8] Spectrograms were interpreted by comparing with standard plates showing the dilution spectra of the various elements. These plates were loaned and the interpretations of the spectrograms checked by Dr. Theodore Kennard.

Pink tourmaline, when heated in a crucible to about 550°C. was found to turn colorless. This change appears to be fairly rapid and in all cases where crystals were heated the color was constant throughout, no zoning becoming apparent. When powdered portions were given the same treatment the change was not so rapid or complete, some of the pink coloring remaining even after longer periods of heating. This result might be explained on the following basis. Holden[6] considers that certain pink minerals, including quartz and rubellite, are colored by trivalent manganese. Divalent and tetravalent manganese were not believed to be significant in this respect. Assuming this to be the case and if the decoloration is a reducing process, then upon heating in air a powder would be less likely to change than a solid crystal.

Using samples of rose quartz which had been heated until they were colorless, Holden[6] subjected the specimens to radium radiation. On such exposure the quartz regained some of its pink coloration. Doelter[4] found that white tourmaline exposed to radium radiation also assumed a faint pink. In this work, the pink tourmaline changed to colorless at about 560°C. In view of the similarity between these experiments, it might be safe to assume that manganese is partly responsible for the color of pink and red tourmaline. This assumption that manganese is responsible for the pink coloration has not yet been definitely established, but as manganese was present in every sample tested, it is certainly a possibility. Further investigation in the field of absorption spectroscopy will be necessary to verify this potential possibility.

Li, Na, Mg, Ca, Al, B, and Ga were found to remain nearly constant in all the samples tested. In the cases where the amounts varied, the variation did not coincide with differences of color. Therefore, it would seem apparent that these elements are not responsible in themselves for color variation. Tin was slightly more pronounced in pink than in green, and copper was more common in green than in pink. The following elements were found to be present in every case when tested for: Li, Na, Mg, Ca, Al, B, Mn, Si, and V. K, Cu, Fe, Pb, Sn, Ti, and Be were found in some samples, but not in all. Ag, Ge, Re, As, Hf, Rh, Sb, Ru, Bi, Hg, Sc, Au, In, Ta, Ir, Te, Cb, La, Th, Cd, Mo, U, Ce, Ni, W, Co, P, Yt, Pd, Zn, and Pt were tested for and not found.

In view of the facts obtained, let us assume that the natural color of tourmaline is either pink or red. Pink and red crystals, when subjected to heat, become colorless. Iron in tourmaline changes the natural pinks to greens. Scharizer[9] definitely states that with increasing manganese content color shifts from blue through green to red. There appeared to be a tendency towards this relationship in the samples tested with the spectrograph. Riggs[2] found that, while the lithia tourmalines contain more or less manganese and give red, green, blue and colorless crystals, the shades of color were not dependent on the absolute amount of manganese present but rather on the ratios existing between that element and iron. When the ratio Mn:Fe was approximately 1:1, pink, colorless, or very pale green resulted. An excess of Mn produced red variation, and where iron was the predominating element of the two, various shades of green resulted. In the author's work, this ratio relationship was found to exist in practically every case and appears to have an extremely important bearing on color change. The depth of green is due to the intensity of iron concentration, while variation in the blue and bluish greens may be due to changes of copper content, the blues having lower concentration than the yellow greens, which are the highest. Purple and lavender tourmaline may be the result of valence changes in iron. It is known that ferrous or ferric iron may be responsible for either green or reddish colorations. Holden[6] found the amethyst color in purple quartz due to iron. The correlation between composition and color in the cases of different colored portions of bi-colored crystals was identical with that of single crystals of the corresponding colors.

Due to the accuracy of spectrographic investigation, it is felt that the results obtained have disproved statements to the effect that magnesium is responsible for color changes. In an examination of red tourmaline Wild[1] considered Ga to be a possible pigment, but failed to find any trace of Mg. In the material which was examined spectrographically, however, the Mg remained constant in both red and green experiments. Contradictory data on heat discoloration is discussed by Doelter.[4] From the recorded observations there is an indication that iron is one, and possibly the most important, factor in gem coloration. In this connection, it is interesting to note that Papish[10] found iron to be the significant pigment in rubies.

[9] Scharizer, *Z. Kryst.*, vol. **15**, p. 355, 1889.

[10] O'Leary, Roger, and Papish, *Science*, vol. **80**, pp. 412-414, 1934.

THE OCCURRENCE OF MENDOZITE AND TAMARUGITE IN MISSOURI

W. D. Keller, *University of Missouri, Columbia, Missouri.*

Introduction

During the second week of June, 1934, the writer collected from an outcrop of Joachim dolomite near the town of Eureka, Missouri, a hydrous soda alum efflorescence which was found to be composed largely of mendozite with some tamarugite. A similar substance, later identified as the same minerals, occurred as an efflorescence on the basal Cherokee conglomerate at Fulton, Callaway County, Missouri. Mendozite has been reported at Mendoza and elsewhere in Argentina, in Chile, at the solfatara of Pozzuoli near Naples, and in Box Elder County, Utah, but never before, to the writer's knowledge, from Missouri.

Occurrence and Description

The mineral of the St. Louis County locality occurred as a white, fluffy to granular powder in varying degrees of compactness on the west-facing side of a recently excavated road cut in the Joachim dolomite on the Woods Road about one mile north of Eureka, Missouri. A section of dolomite about 10 feet in thickness and fifty yards long is exposed in the cut which lies low on a west sloping hillside. Ground water migrating down the slope of the hill and seeping out on this surface would be dried by the mid-day and afternoon sunshine. The evaporating water, fed by seepage and capillarity, would leave behind its soluble load as a residue on the surface. This deposited on the limestone surface as a white powdery coating, thickening to a friable porous encrustation up to about 3/8 inch in thickness, or hanging in fragile little stalactites as much as $\frac{1}{2}$ inch in length below the narrow bedding plane shelves.

No apparent relationship could be established between the efflorescence and slope wash markings, porous beds or impervious layers in the limestone. Apparently the freshest-appearing part of the limestone carried the thicker or more abundant efflorescence. In fact, the margin of the deposit outlined a profile of freshness on the limestone.

A generous sample was scraped from the thicker crusts and stalactites. It had a slightly astringent, stinging taste.

The powdered efflorescence was examined microscopically and the material other than impurities of fine quartz, dolomite, and clay, was found to consist of two different substances, both being anisotropic. One had low birefringence, was extremely fine-grained, occurred in small aggregates, and had a general index of refraction that varied but slightly from 1.490. It was so fine-grained that no other optical properties could be determined. The other anisotropic material was highly birefringent and varied in index of refraction between 1.430 and 1.460. A few grains were found which gave slightly uncentered acute bisectrix figures and the mineral was found to be unquestionably biaxial negative, with an estimated axial angle of about 40°. The beta index was near 1.450 although the exact value was not obtained. Because of the fineness of grain (magnifications up to 1200 *X* were used) and partial contamination of borders by clay, very precise values of the optical properties could not be determined.

However, reference to Larsen and Berman's determinative tables[1] suggested that the mineral was mendozite, $Na_2O \cdot Al_2O_3 \cdot 4SO_3 \cdot 22H_2O$. Accordingly, a distilled water solution of the efflorescence was made and allowed to evaporate to dryness and the crystallized product studied optically. It was comparatively coarsely crystalline and determined to be mendozite with the following optical properties: $\alpha = 1.436$, $\beta = 1.455$, $\gamma = 1.459$, $\pm .003$; biaxial, negative, $2V = 40°–50°$, dispersion, $r > v$, $X = b$. The similarity of these data with those obtained on the original or undissolved material is believed to be confirmatory of the identification of one of the efflorescence minerals as mendozite.

The following chemical tests are likewise in accord. The material was soluble in cold distilled water except for a small amount of buff-colored residue determined microscopically to be dolomite and quartz. The filtered solution gave stong positive qualitative tests for the sulfate ion and aluminum, but negative micro-chemical tests for potassium and chloride. The flame color test for potassium on the solid material was likewise negative. These are the results one would expect for mendozite. A test for iron was negative, eliminating halotrichite as a possibility.

Larsen reports that mendozite alters in air to tamarugite, $Na_2O \cdot Al_2O_3 \cdot 4SO_3 \cdot 12H_2O$, which has indices of refraction as follows:

---

[1] The Microscopic Determination of the Non-Opaque Minerals, *U. S. Geol. Survey*, Bull. **848.**

$\alpha = 1.484$, $\beta = 1.487$, $\gamma = 1.496$. The writer believes that the very fine-grained mineral having indices of refraction near 1.490 is tamarugite coming from the alteration of mendozite. Positive identification was impossible because of the fineness of grain.

An efflorescence similar in appearance to the one described but not studied closely had been noticed two years before on a large south-facing outcrop of very coarse conglomerate forming the north bank of Stinson Creek in the southeast part of Fulton, Missouri. This locality was revisited in November, 1934, and material collected for study. The denser crusts and coarser particles gave the same chemical and optical results as the St. Louis County material. The finest filaments associated with the efflorescence were too small to be measured optically except that their indices fell within the range of the coarser material. It is believed that this efflorescence is likewise mendozite.

ORIGIN OF THE MENDOZITE

In accounting for the probable origin of the constituents of mendozite on the Joachim dolomite it seems most logical that the source of the sulfate was oxidizing pyrite. The insoluble residue in HCl contains fine-grained pyrite, clay which is limonite-stained, and a little fine quartz sand. Sulphuric acid released from the oxidized pyrite might react with the clay to form an aluminum sulfate. Sodium may have come from sodium clay in the dolomite or it may have been present as a remnant of connate waters. The development of the efflorescence on the freshest part of the exposure suggests that at least one of the essential constituents is associated with unweathered rock.

REMOVAL OF BUBBLES FROM OLD THIN-SECTIONS OF ROCKS

W. D. Keller, *University of Missouri.*

During a recent examination of a number of thin-sections of sedimentary rocks some were found to contain so many bubbles that the sections could not be studied effectively or photographed satisfactorily. Their removal presented a serious problem. It was impossible to melt the cement or transfer the rock-slice without losing the section because the sediments were so poorly indurated that they would "wash away" as soon as the cement was melted or moved.

Whether the bubbles developed through age or faulty technique in preparation is not known, but they were present in both Canada balsam and kollolith mounts. They occurred either above or below (or both) the rock-slice.

The following treatment was successfully used, however, in removing about ninety per cent of the bubbles—enough to save the sections.

The cover glass was taken off the section, starting with a gentle prying action at a place appearing most favorable.

Commonly the cover could be lifted off intact, made possible probably because of the abundance of bubbles and poor adherence. Then a few drops of xylol were run onto the slice and cement, and after standing a few minutes were allowed to drip off. By repeating this process several times the excess cement was dissolved and under-slice bubbles probably filled. At any rate, they disappeared. The section was laid away to dry thoroughly after which the clean cover glass was remounted using the kollolith in xylol[1] solution for that purpose and allowed to harden. Apparently the section was as good as new.

---

[1] Sold by Voigt and Hochgesang, Göttingen, Germany.

NEW MINERAL NAMES

Herzenbergite

PAUL RAMDOHR: Nordenskiöldin in einer zinnerzlagerstätte (Nordenskioldine in a tin deposit). *Jahr. Min., Beil. Bd.*, Abt, **A**, p. 293, 1934.

The name herzenbergite is proposed for the tin sulfide described under the name kolbeckine. (Cf. *Am. Mineral.*, vol. **18**, p. 223, 1933).

W. F. F.

Orthoguarinite, Clinoguarinite

G. CESÁRO: Sur la guarinite. *Mem. Acad. Roy. Belg. Cl. Sci.*, vol. **12**, fasc. 3, p. 18, 1932.

Cesáro believes guarinite to be a distinct mineral with monoclinic crystallization (clinoguarinite) but often orthorhombic (orthoguarinite) through superposition of hemitropic lamellae of the monoclinic mineral.

W. F. F.

Chrome-nontronite

D. P. SERDIUCHENKO: Chrome-nontronites and their genetical relationships with the serpentines at the Northern Caucasus. Zap. Ross. Min. Obshch. (*Mem. Soc. Russe Min.*) Ser. 2, vol. **62**, pp. 376–391, 1933. Russian with English summary.

CHEMICAL PROPERTIES: Analyses (from Bolshaia-Laba river) SiO_2 46.09, TiO_2 1.04, Al_2O_3 24.04, Cr_2O_3 1.12, Fe_2O_3 3.96, FeO 0.33, MnO 0.49, NiO trace, CaO 1.86, MgO 6.99, H_2O (−) 5.67, H_2O (+) 7.26, total 98.85; (from Gedmyshkh Valley) SiO_2 36.69, Al_2O_3 16.77, Cr_2O_3 3.76, Fe_2O_3 8.70, CaO 2.57, MgO 1.60, H_2O (−) 8.42, H_2O (+) 12.90, total 99.24.

OCCURRENCE: Found as emerald green pebbles in conglomerates along the upper course of the Bolshaia-Laba River or as a green colored clay above serpentine or cementing sandstone in the Gedmyshkh and Cheghet-Lakhran valleys, North Caucasus.

W. F. F.

Chrome-beidellite

D. P. SERDIUCHENKO: *Ibid.*

CHEMICAL PROPERTIES: Analysis: (from Cheghet-Lakhran) SiO_2 43.14, TiO_2 0.96, Al_2O_3 16.07, Cr_2O_3 5.02, Fe_2O_3 4.70, FeO 0.61, MnO 0.21, NiO 0.30, CaO 1.46, MgO 3.45, P0.01, S 0.15, H_2O (−) 16.66, H_2O (+) 7.32, sum 100.06.

OCCURRENCE: Found as an olive green clay above serpentine at Cheghet-Lakhran Valley, North Caucasus.

W. F. F.

PROCEEDINGS OF SOCIETIES

PHILADELPHIA MINERALOGICAL SOCIETY

The Academy of Natural Sciences of Philadelphia, March 7, 1935.

President Joseph L. Gillson presided at a stated meeting of the society, 42 members and 30 visitors being present.

Dr. Clarence S. Ross addressed the society on "The Clay Minerals and their Methods of Study" with lantern slide illustrations. He divided the clay minerals into two groups: the kaolinite group and the montmorillonite group. Clays are typical one-dimensional colloids, although a large proportion of the clay minerals in soils are not colloidal in size. All are platy in habit. They may be differentiated by their *X*-ray patterns. Dana gave species rank to amorphous allophane. The name mineraloids was proposed for such materials of no fixed composition.

Mr. M. C. Towns, a visitor, exhibited cut and uncut emerald from Colombia.

April 4, 1935

A stated meeting was held on this date, with Dr. Gillson in the chair; 130 members and visitors being present.

Mr. W. D. B. Motter Jr. talked on "Copper as mined by the Chile Exploration Company at Chuquicamata," illustrated with five reels of motion pictures. The orebody, the largest copper orebody in the world, is $1\frac{3}{4}$ miles long, $\frac{1}{4}$ mile wide, and 1900 feet thick. The principal minerals are brochantite, chalcanthite, atacamite, krohnkite, chalcocite, and enargite. There are reserves of a billion tons of ore, averaging 2% copper. Specimens were exhibited.

W. H. Flack, *secretary*

Edward Salisbury Dana, Professor emeritus of physics at Yale University and honorary life fellow of the Mineralogical Society of America, died on June 16, in his eighty-sixth year.